

UNIVERSITA' DEGLI STUDI DI NAPOLI "FEDERICO II"

Scuola di Medicina e Chirurgia



TESI DI DOTTORATO DI RICERCA IN

TERAPIE AVANZATE BIOMEDICHE E CHIRURGICHE XXX CICLO

Triennio accademico 2014-2017

**Neutrophil extracellular traps (NETs) in cancer-associated thrombosis and
tumor progression: role of integrins $\alpha 5\beta 1$, $\alpha v\beta 3$ and $\alpha IIb\beta 3$**

Tutor: Ch.mo Prof. Giovanni Di Minno

Candidato: Dr. Marcello Monti

Co-Tutor: Ch.ma Prof.ssa Silvana Del Vecchio

INDEX

SUMMARY	2
INTRODUCTION	
<i>Defensive properties and functions of neutrophils</i>	4
<i>Neutrophil extracellular traps (NETs)</i>	6
<i>NETs in infection and inflammation</i>	7
<i>NETs in thrombosis</i>	8
<i>NETs and cancer</i>	10
<i>Integrins</i>	11
AIM OF THE STUDY	14
MATERIALS AND METHODS	
<i>Differentiation of HL-60 cells and NETs production</i>	15
<i>Cell lines for adhesion assays</i>	16
<i>FACS analysis of integrin and antigen expression</i>	16
<i>Western blot analysis of integrin expression</i>	17
<i>Qualitative and quantitative analysis of NETs</i>	17
<i>Analysis of NETs protein components</i>	18
<i>Co-immunolocalization studies by confocal microscopy</i>	19
<i>Cell adhesion assays to NETs</i>	19
<i>Statistical analysis</i>	21
RESULTS	
<i>Characterization of neutrophil-like cells and NETs production</i>	21
<i>Expression and co-immunolocalization of NETs markers</i>	22
<i>Adhesion of $\alpha 5\beta 1$ and $\alpha v\beta 3$ expressing cells to NETs</i>	22
<i>Fibronectin is a protein component of NETs</i>	24
<i>Integrin-dependent adhesion to NETs of different cancer cell lines</i>	26
DISCUSSION	27
REFERENCES	30
TABLES	39
FIGURES	40

ABBREVIATIONS

NETs	<i>neutrophil extracellular traps</i>
ROS	<i>reactive oxygen species</i>
MPO	<i>myeloperoxidase</i>
NE	<i>neutrophil elastase</i>
fMLP	<i>formyl-Met-Leu-Phe</i>
PAD4	<i>peptidylargininedeiminase 4</i>
ECM	<i>extracellular matrix</i>
PMA	<i>phorbol 12-myristate 13-acetate</i>
G-CSF	<i>granulocyte colony-stimulating factor</i>
Cit H3	<i>citrullinated histone H3</i>
uPAR	<i>urokinase plasminogen activator receptor</i>
MMP	<i>matrix metalloproteinase</i>
vWF	<i>von Willebrand factor</i>
HBSS	<i>Hank's balanced salts solution</i>
PBS	<i>phosphate-buffered saline</i>
CM	<i>conditioned medium</i>

SUMMARY

Upon infection of pathogens, neutrophils are the first white blood cells activated to entrap and kill invading microorganisms through the processes of phagocytosis or degranulation. A newly discovered mechanism used by neutrophils to eliminate bacteria, viruses and fungi is the release of neutrophil extracellular traps (NETs), web-like structures composed of nucleic acids, histones and selected cytoplasmic proteins, like myeloperoxidase and neutrophil elastase. In addition to their main defensive function, NETs were reported to promote thrombotic events and metastatic dissemination of cancer cells, but the mechanisms underlying these processes have not been elucidated yet. In this PhD thesis project, we tested the role of $\alpha 5\beta 1$, $\alpha v\beta 3$ and $\alpha IIb\beta 3$ integrins in the adhesion of different human cancer cell lines using cell-free isolated NETs as substrate. Neutrophil-like cells, obtained after differentiating HL-60 cell line with DMSO, were stimulated with calcium ionophore A23187 and used as a stable source of NETs. Two human leukemia cell lines, differentially expressing $\alpha 5\beta 1$ and $\alpha v\beta 3$ integrins, were subjected to adhesion assays in the presence or absence of DNase 1, blocking antibodies against $\alpha 5\beta 1$ or $\alpha v\beta 3$, alone or in combination with DNase 1, and Proteinase K. As expected DNase 1 treatment strongly inhibited adhesion of both cell lines to NETs. An equivalent significant reduction of cell adhesion to NETs was obtained after treatment of cells with blocking antibodies against $\alpha 5\beta 1$ or $\alpha v\beta 3$ indicating that both integrins were able to mediate cell adhesion to NETs. Furthermore, the combination of DNase 1 and anti-integrin antibody treatment almost completely blocked cell adhesion. Western blot analysis and immunoprecipitation experiments showed a dose-dependent increase of fibronectin levels in samples from stimulated neutrophil-like cells and a direct or indirect interaction of fibronectin with histone H3. Co-immunolocalization studies with confocal microscopy showed that fibronectin and citrullinated histone H3 co-localize inside the web-structure of NETs. Then, we screened a panel of human cancer cell lines endogenously expressing different protein levels of $\alpha 5\beta 1$, $\alpha v\beta 3$ and $\alpha IIb\beta 3$ integrins in the adhesion to NETs: the concomitant expression of $\alpha 5\beta 1$,

$\alpha v\beta 3$ and $\alpha IIb\beta 3$ integrins was associated to an enhanced adhesion to NETs and the addition of an excess of cyclic RGD peptide inhibited cell adhesion at a different extent in each cell line. Interestingly, the maximal reduction of integrin-dependent adhesion to NETs was similar to that obtained after DNase 1 treatment, confirming that both DNA and fibronectin determined cell attachment to NETs. Since low or undetectable levels of $\alpha 5\beta 1$ integrin prevents cell adhesion to NETs, this integrin is need to anchor cells in the web-like structure of NETs, allowing a close interaction between cells and DNA/histone complexes.

This PhD thesis demonstrated that $\alpha 5\beta 1$, $\alpha v\beta 3$ and $\alpha IIb\beta 3$ integrins modulate cell adhesion to NETs by binding to their common substrate fibronectin, found to be a protein component of NETs. In addition to mechanical trapping, integrin-mediated cell adhesion to NETs should be taken into account as a mechanism promoting cell-cell interactions at the interface with NETs. Therefore, by using integrins-specific antibodies or the RGD cyclic peptide is possible impairing the homing of different integrins-expressing cell types such as platelets, endothelial and cancer cells to specific sites of NETs accumulation, thus reducing NETs-dependent cancer-associated thrombosis and tumor progression.

INTRODUCTION

Defensive properties and functions of neutrophils

In humans, neutrophils or polymorphonuclear cells (PMNs) account for 50% to 70% of all circulating leukocytes and represent the first line of host defense against invading pathogens [1]. Mature neutrophils are released from the bone marrow in a highly regulated manner [2] and circulate in the blood as cells with a segmented nucleus and a cytoplasm enriched with granules and secretory vesicles. In response to infection, circulating neutrophils migrate towards invading pathogens in an ordered multistep process referred to as neutrophil recruitment. The initial steps of this process are the attachment of free-flowing neutrophils to the surface of the endothelium (capture) and their rolling along the vessel in the direction of blood flow [3]. These events are mainly mediated by the low-affinity dynamic interactions of selectins receptors on endothelial cells with their ligands on neutrophil surface. The subsequent step is the adhesion of rolling neutrophils to the endothelium. Chemokines immobilized on the luminal side of endothelium activate neutrophils thus inducing conformational changes of neutrophil surface integrins allowing them to interact with ligands expressed on the inflamed endothelium. The binding of integrins with their extracellular ligands activates signaling pathways inside the neutrophil thus stabilizing adhesion and initiating cell motility. While remaining firmly attached to the endothelium, neutrophils start to crawl searching for the preferential site of transmigration. Crawling neutrophils actively move towards endothelial junctions and this process mainly depends on the $\beta 2$ integrin macrophage 1 antigen (MAC-1) [4, 5]. Once neutrophils reach their extravasation site by intraluminal crawling, they have to cross the endothelial cell layer, the basement membrane and pericytes to enter the interstitial tissue. Endothelial transmigration requires integrins and multiple adhesion molecules and may occur via a paracellular (between endothelial cells) or transcellular (through an endothelial cell) route. The paracellular transmigration is usually preferred by neutrophils that reach the basement membrane in a few minutes. Although neutrophils have specific proteases that may digest

ECM proteins, they cross the basement membrane mainly by migration through less dense regions with low levels of ECM proteins. Finally, neutrophils migrate through the pericyte network by crawling along the cells and searching for permissive gaps between adjacent cells that allow them to leave the vasculature [3, 6, 7].

Once in the interstitial tissue, neutrophils need to find the site of infection where they can eliminate the invading pathogens. This is accomplished by site-directed migration of neutrophils in response to a chemotactic gradient, a process termed chemotaxis. Previous studies showed that there is a hierarchy of chemotactic molecules in an infected tissue [8, 9]. The chemoattractant molecules derived from bacterial products such as formyl-Met-Leu-Phe (fMLP) (end-target chemoattractant) dominate over other chemotactic stimuli released at intermediary sites (intermediate chemoattractant). Among all these migratory stimuli, neutrophils preferentially respond to end-target chemoattractants so that interfering signals from local environment do not deviate them from the final destination.

At the infectious site, neutrophils kill pathogens by essentially three mechanisms: phagocytosis, degranulation and release of neutrophil extracellular traps (NETs). During phagocytosis, the pathogens are firstly recognized and opsonized by engagement of specific receptors/antigens and then enclosed in a defined vacuole. Uptake is followed by fusion of the phagocytic vacuole with preformed granules containing NADPH oxidase subunits and hydrolytic enzymes. Finally, pathogens are killed by reactive oxygen species (ROS) generated by the activation of NADPH oxidase and exposure to proteinases and anti-microbial peptides such as cathepsins, defensins, lactoferrin and lysozyme. Furthermore, fusion of granules with the plasma membrane allows the release of antibacterial proteins into the extracellular space where they can act against extracellular pathogens. A third mechanism of extracellular bacterial killing is the formation and release of neutrophil extracellular traps by activated neutrophils. This process has been recently identified [10] and rapidly became a hot topic in research areas exploring not only the defensive properties of neutrophils but also their role in different pathological conditions.

Neutrophil extracellular traps (NETs)

NETs are web-like structures released from activated neutrophils exposed to different pathogens including bacteria, virus or fungi. They are composed of decondensed chromatin associated with histones and other granular proteins such as myeloperoxidase (MPO), neutrophil elastase (NE), several antimicrobial peptides and matrix metalloproteinases 8, 9 and 25 (MMP8, MMP9 and MMP25) [3, 10-12]. The main function of NETs is the entrapment of pathogens and inactivation of their virulent factors through enzymatic degradation [13-17].

The release of NETs occurs through a multistep process termed NETosis. In the first phases of this process, specific morphological changes can be observed in neutrophils including chromatin decondensation and loss of the classical lobulated nuclear morphology, disruption of nuclear membrane and subsequent mixing of nuclear and cytoplasmic content followed by extrusion into extracellular environment through plasma membrane disintegration [12, 18]. The process is also characterized by several biochemical changes including activation of peptidylargininedeiminase 4 (PAD4), an enzyme that induces citrullination of histones, along with increased activity of MPO and NE [13-15, 18, 19]. It has been proposed that chromatin decondensation is primarily driven by histone citrullination since inhibition or knock-down of PAD4 impairs the ability of neutrophils to release NETs [20, 21]. Upon activation, NE was reported to translocate from cytoplasmic granules to the nucleus where it contributes to histone cleavage [19]. MPO also contributes to the decondensation of nuclear DNA and disruption of nuclear membrane even though this process was not completely elucidated. Due to their critical role in NETosis, citrullinated histones, MPO and NE are considered the major biomarkers of NETs associated with extracellular double-stranded DNA. At the end of the process, the release of NETs and the disruption of plasma membrane usually leads to cell death and loss of viable cell function such as migration and phagocytosis. It has recently been reported that certain NETosis-inducing stimuli may trigger neutrophils to release NETs by blebbing of the nuclear envelope and vesicular exportation [18, 21, 22]. In this case, the preserved

integrity of plasma membrane allows the neutrophil to remain viable and to retain several functions such as migration. This type of NETs release is termed vital NETosis as opposed to suicidal NETosis.

In addition to bacteria, virus and fungi, different chemical compounds such as calcium ionophore A23187, phorbol 12-myristate 13-acetate (PMA) and potassium ionophore nigericin can stimulate neutrophils to release NETs. Some authors reported that calcium ionophore A23187 was more efficient and rapid than PMA to induce NETs release [13, 23].

NETs in infection and inflammation

A number of pathogens can stimulate neutrophils to release NETs. Several bacterial molecules including the cell surface components LPS, lipoteichoic acid and their breakdown products are potent inducers of NETs. Bacteria are suggested to be entrapped by NETs due to the electrostatic interaction between the positively charged bacterial surface and the negatively charged chromatin fibers [24]. After entrapping, NETs are reported to disarm and inactivate bacteria mainly through the enzymatic activity of neutrophil elastase and the antimicrobial activity of histone and histone-derived peptides [25]. Both Gram-positive and Gram-negative bacteria including *Staphylococcus aureus*, *Salmonella typhimurium* and *Shigella flexneri* can be entrapped by NETs. Similarly, *Escherichia coli* and *Pseudomonas aeruginosa* can be immobilized and eliminated by NETs [26]. The microbicidal activity of NETs against different pathogens results from the combined action of several components showing an enhanced effects due to their high local concentration on the NETs' surface. For instance, NETs are reported to contain calprotectin, a cytosolic protein capable of disarming and killing *Candida albicans* [12]. The antifungal activity of NETs has been also assigned to calgranulin which chelates zinc, a cation required for fungal growth [24] and NETs toxicity for *Aspergillus fumigatus* and *Cryptococcus neoformans* was ascribed to this mechanism [26, 27]. Among other pathogens, NETs are able to eradicate several viruses mainly through the

MPO and defensins activity. MPO has a direct anti-viral effect against HIV-1 and cytomegalovirus while defensins have multiple modes of action especially against respiratory viruses like influenza A and RSV [26-28].

The release of NETs by activated neutrophils may also have detrimental effects on the host. A panel of self molecules are exposed extracellularly on the surface of NETs and this may trigger a harmful inflammatory autoimmune response [29, 30]. NETs were detected in renal and skin biopsies of patients with systemic lupus erythematosus, an autoimmune disease characterized by the formation of auto-antibodies against chromatin and neutrophil components [31]. It was proposed that a high levels of cytokines such as TNF- α and IFN- α sensitize neutrophils to release NETs in response to anti-proteinase 3, anti-ribonucleoprotein, anti-defensin, or anti-LL-37 autoantibodies [32-34]. Furthermore, NETs are reported to be involved in the pathogenesis of other autoimmune diseases including rheumatoid arthritis [35], psoriasis [36, 37] and some types of vasculitis [7].

NETs in thrombosis

Extensive evidences indicate that NETs have a relevant role in coagulation and thrombus formation since NETs can provide a scaffold for platelet and red blood cell adhesion and aggregation thus enhancing coagulation [38-40]. Biomarkers of NETs have been found in thrombi and plasma of both animal models and patients with deep venous thrombosis [38, 41]. Previous studies reported that NETs might promote thrombosis in different ways [15]. Several plasma proteins important for platelet adhesion and thrombus propagation such as fibronectin and von Willebrand factor may bind to NETs [40]. The major constituents of NETs, DNA, histones and proteases, all have procoagulant properties. Nucleic acids activate coagulation with RNA binding to both factor XII and XI in the intrinsic pathway [42, 43]. Histones increase thrombin generation in a platelet-dependent manner [44, 45]. Histones activate platelets and platelet activation, in turn, promotes coagulation. In addition, histones are cytotoxic to the endothelium and can induce macro and microthrombosis in

vivo. Serine proteases, such as neutrophil elastase, was shown to inactivate tissue factor pathway inhibitor (TFPI) through cleavage thus resulting in an increased procoagulant activity with consequent platelet activation and enhanced NETs formation. Massberg et al showed that thrombus formation in response to arterial vessel injury was reduced in mice deficient in neutrophil elastase and cathepsin G as compared to wild type animals [46]. In animal models of deep venous thrombosis, treatment with DNase 1 that degrades NETs resulted in a significantly lower frequency of thrombus formation [38, 47]. In PAD4-deficient mice, the impaired production of NETs resulted in a strongly reduced formation of thrombi following inferior vena cava stenosis [48]. Interestingly, the PAD4-deficient mice retain normal tail bleeding time suggesting that NETs do not affect platelet plug formation in response to a small injury but they may have a critical role in the stabilization of thrombi in large vessels. This implies that targeting PAD4 for prevention of thrombosis would not likely cause spontaneous hemorrhages.

The association between cancer and thrombosis is well established. An approximately 4-fold increased risk of venous thromboembolism has been reported for cancer patients as compared to general population [49]. Pancreatic and brain cancer patients have a higher risk of venous thromboembolism than breast and prostate cancer patients. Moreover, patients with metastatic disease have a higher risk than those with localized tumors [49]. Many factors including tissue factor, microparticles, cytokines, soluble P-selectin, elevation in coagulation factors, secretion of mucins, thrombocytosis and leukocytosis were involved in the prothrombotic state associated with cancer. Recently Demers et al investigated the role of NETs in lung thrombosis in two mouse tumor models [50]. An increased number of peripheral blood neutrophils was found in tumor-bearing animals and these neutrophils were more prone to release NETs as compared to those derived from healthy animals. The same authors reported that tumor-derived granulocyte colony-stimulating factor (G-CSF) was responsible for the neutrophilia and NETs release. Finally, hypercitrullinated histone H3, the main biomarker of NETs, was detected in thrombi in the lungs of these tumor-bearing mice.

NETs and cancer

Patients with various tumor types, including breast, lung and colorectal cancer often exhibit an increased number of neutrophils in peripheral blood [1]. In addition, the relative frequency of immature neutrophils is increased in certain types of cancer and this may be due to a tumor-induced emergency granulopoiesis in response to upregulation of several cytokines and chemokines. It is well established that neutrophils are recruited to tumor sites where they constitute a significant portion of inflammatory cell infiltrate and they may have both pro and anti-tumoral properties [51]. Neutrophils may exert pro-tumoral activity by different mechanisms, including the development of chronic inflammation, an enhanced tumor angiogenesis and modulation of cell migration and invasion. A high levels of tumor-infiltrating neutrophils are associated with advanced disease and poor clinical outcome in cancer patients [52-54]. Previous studies also showed antitumor activity of neutrophils. A number of antimicrobial mediators expressed by neutrophils such as defensins, proteases, myeloperoxidase, and reactive oxygen species may have potent tumor-cytotoxic activity. Furthermore, neutrophils also express cytokines, chemokines, and growth factors with the potential to recruit and activate cells of the innate and adaptive immune system [55-57]. Neutrophils may also release NETs at tumor site and the mechanisms by which they are formed and influence tumor microenvironment are not known.

Previous studies reported the presence of NETs in Lewis lung carcinomas at sites of neutrophil accumulation especially in areas of apparent necrosis [58]. A similar pattern was observed in histological sections of human Ewing sarcoma [59].

The involvement of NETs in promoting metastasis has been recently investigated. In a model of systemic infection, Cools-Lartigue et al demonstrated microvascular depositions of NETs and consequent trapping of circulating lung carcinoma cells within DNA webs. NETs trapping was associated with increased formation of hepatic micrometastases at 48 hours and gross metastatic lesions at 2 weeks following tumor cell injection. These effects were abrogated by NETs inhibition

with DNase 1 or neutrophil elastase inhibitor [60]. In an experimental mouse model, breast cancer cells induced neutrophils to release NETs in the absence of infection. NETs were detected by intravital microscopy around metastatic cancer cells in lung tissue and mice treated with DNase 1-coated nanoparticles showed reduced experimental metastases [61]. In a mouse model of sepsis, a condition promoting NETs deposition in liver sinusoid and lung capillaries, the intrasplenic injection of A549 cancer cells expressing β 1-integrin resulted in their adhesion to hepatic sinusoids as assessed by intravital microscopy. Silencing of β 1-integrin with targeted siRNA in cancer cells before injection caused a decrease of cell adhesion to NETs in liver sinusoids [62].

Integrins

Integrins are transmembrane heterodimeric receptors composed of non-covalently associated α and β subunits, which integrate the extracellular matrix with the intracellular cytoskeleton to mediate cell migration and adhesion. A property of most integrins is their ability to bind a large spectrum of ligands. Furthermore, many extracellular matrix and cell surface adhesion proteins may bind to multiple integrin receptors. Several members of integrin superfamily bind to their extracellular ligands through the recognition of the tripeptide Arg-Gly-Asp (RGD). This motif was originally identified in fibronectin and subsequently it was found in many other protein components of the extracellular matrix (ECM) including vitronectin, von Willebrand factor, osteopontin, fibrinogen and laminin. The RGD motif can be recognized by different integrins including α 5 β 1, α v β 3, α v β 5 and α IIb β 3 [63-65].

Integrins are expressed on the plasma membrane in an inactive status in which they do not bind their ligands and do not transduce signals unless exposed to activating stimuli. Activation occurs through an “outside-in” and “inside-out” signaling that result in conformational changes that in turn increase the ligand-binding affinity. Integrin ligation by its own natural ligands triggers a signaling cascade in the “outside-in” direction by oligomerization and co-clustering with kinases and adaptor

proteins such as focal adhesion kinase and Src and by activating a number of intracellular mediators. The “inside-out” signaling occurs when intracellular signals induce dissociation of the α and β transmembrane domains and cytoplasmic tails followed by conformational changes and generation of a high affinity binding integrin [66].

Among members of the integrin family, a prominent role in angiogenesis and metastatic dissemination is played by $\alpha v\beta 3$, $\alpha v\beta 5$ and $\alpha 5\beta 1$. Overexpression of these integrins is associated with poor prognosis and unfavorable outcomes [66-68]. Integrin $\alpha v\beta 3$ is strongly upregulated at transcriptional level by pro-angiogenic growth factors or chemokines in activated endothelial cells. Expression and activation of this integrin was also found to be correlated with tumor invasion and metastases in melanomas, gliomas, ovarian and breast cancer. In particular, activated $\alpha v\beta 3$ is reported to cooperate with metalloproteinase and to strongly promote metastasis in human breast cancer cells [69, 70]. Although less extensively studied, also $\alpha v\beta 5$ is reported to be involved in tumor invasion and metastases in a variety of malignant tumors mainly of epithelial origin. In this respect, $\alpha v\beta 5$ physically interacts with urokinase plasminogen activator receptor (uPAR) promoting proteolytic disruption of ECM, dysregulation of cell adhesion properties and urokinase-dependent cell migration in breast cancer [71].

Expression of $\alpha 5\beta 1$ is strongly induced upon hypoxia and promotes tumor metastasis in breast cancer. Breast cancer cells with high $\alpha 5\beta 1$ levels revealed a 3-fold increased cell invasiveness, compared with cells exhibiting low $\alpha 5\beta 1$ expression [72]. Furthermore high $\alpha 5\beta 1$ expression in clinical biopsies is associated with an increased risk of mortality. Previous studies reported that $\alpha 5\beta 1$ integrin mediates neovascularization and aggressiveness through an increase of MMP-9 activity in solid tumors like glioblastoma, melanoma and ovarian cancer [73, 74]. Mice injected with $\alpha 5$ -silenced Lewis lung cancer cells showed lower burden of implanted tumors, and a dramatic decrease in lung metastases resulting in higher survival as compared with mice injected with wild-type cells [75]. Integrins $\alpha v\beta 3$ and $\alpha 5\beta 1$ are reported to cooperate in different biological processes

such as regulation of cell contractility and movement, angiogenesis and maintenance of cancer stemness [72].

The integrin $\alpha\text{IIb}\beta\text{3}$ is the most abundant platelet surface receptor and is essential for adhesion, aggregation, and clot retraction. The principal ligand for $\alpha\text{IIb}\beta\text{3}$ is fibrinogen; however, fibronectin, vitronectin and von Willebrand factor (vWF) have also been demonstrated to have the ability to bind the integrin [76]. When fibrinogen or von Willebrand factor are bound to $\alpha\text{IIb}\beta\text{3}$, they can mediate cross bridging with other $\alpha\text{IIb}\beta\text{3}$ receptors on adjacent platelets [77]. Ligand binding to $\alpha\text{IIb}\beta\text{3}$ not only enables platelet–platelet interaction but also transmits an array of signals from the occupied and clustered receptor into the platelet mainly through members of Src family kinases [78-80]. Furthermore, platelet $\alpha\text{IIb}\beta\text{3}$ has been involved in tumor cell-induced platelet aggregation and blockade of this integrin in models of pulmonary metastases reduced the metastatic dissemination of intravenously injected cancer cells [81].

AIM OF THE STUDY

Although a growing body of evidences indicates that NETs are involved in cancer-associated thrombosis and metastatic dissemination, the underlying mechanisms by which NETs mediate such processes and in particular cell adhesion and entrapment of circulating cancer cells have not been elucidated yet. Since integrins are the main mediators of cell adhesion, migration and invasion, we hypothesized that members of integrin family may have a role in promoting cell attachment to NETs. The aim of the present study was to test whether RGD-recognizing integrins such as $\alpha 5\beta 1$, $\alpha v\beta 3$ and $\alpha IIb\beta 3$ may mediate cell adhesion to NETs thus investigating the interplay between cancer cells and neutrophils that may simultaneously promote a procoagulant state and metastatic dissemination.

MATERIALS AND METHODS

Differentiation of HL-60 cells and NETs production

Human HL-60 cell line was maintained in Roswell Park Memorial Institute (RPMI) 1640 supplemented with 10% FBS. These cells have been widely used to study several leukocyte function including oxidative burst, adhesion, chemotaxis and migration [82]. We selected this cell line because upon differentiation it represents an abundant and daily available source of NETs that allowed us to perform adhesion assays avoiding cell-cell interaction and contamination with integrin substrates present in blood samples.

Human HL-60 cells were differentiate into neutrophil-like cells using a standard protocol with slight modifications [83, 84]. Briefly, 1×10^6 HL-60 cells were grown in medium with 1.3% DMSO using T25 flasks in a humidified incubator at 5% CO₂ and 37°C for 5 days adding fresh medium with 1.3% DMSO to the flasks at the third day. Then 1.5×10^6 treated cells were plated into Petri dishes containing 10 ml of fresh medium with 1.3% DMSO to complete differentiation and allow cell attachment for additional 2 days.

To confirm differentiation, changes in cell morphology were assessed by staining with May-Grunwald-Giemsa and the expression of CD11b [85], CD16b [86] and CD177 [87] antigens, markers of neutrophil differentiation, was evaluated by flow cytometry.

To induce the release of NETs, neutrophil-like cells were treated with 2.5 and 25 μ M calcium ionophore (A23187, Sigma-Aldrich) or vehicle. Briefly, differentiated cells were plated onto Petri dishes in RPMI 1640 with or without 10% FBS at a density of 1×10^6 cells/ml and exposed to calcium ionophore for 4 h in a humidified incubator. After treatment, the conditioned medium was recovered and centrifuged at 310xg for 10 min at 4°C to obtain a cell-free NETs-enriched supernatant. This supernatant was then centrifuged at 18000xg for 10 min at 4°C and the pellet containing NETs was resuspended in 100 μ l of cold PBS. Finally, double-stranded DNA concentration was determined using a NanoDrop ND-1000 spectrophotometer with V3.5.2 software

(NanoDrop Technology, Cambridge, UK) and cell-free isolated NETs were used as a stock for further experiments. Different stock suspensions were prepared and used to obtain experimental replicates.

Cell lines for adhesion assays

Human chronic myeloid leukemia K562 cells endogenously expressing $\alpha 5\beta 1$ integrin (K562) and its derived clone, stably cotransfected with cDNA of αv and $\beta 3$ subunits [88], overexpressing $\alpha v\beta 3$ integrin (K562 $\alpha v\beta 3$), were a generous gift of Dr. S.D. Blystone. Cells were grown in Iscove's modified Dulbecco's medium (IMDM) (Gibco Life Technologies) containing 10% FBS [89].

Human fibrosarcoma (HT-1080), glioblastoma (U-87 MG), prostate cancer (DU 145 and PC-3) and epidermoid carcinoma (A-431) cells were grown in Dulbecco's Modified Eagle Medium (DMEM, Gibco Life Technologies) containing 10% FBS whereas non-small cell lung cancer (H1975) were cultured in complete RPMI 1640. All cells were maintained in a humidified incubator at 5% CO₂ and 37°C. Expression of $\alpha 5\beta 1$, $\alpha v\beta 3$, $\alpha v\beta 5$ and $\alpha IIb\beta 3$ integrins were tested by FACS analysis or western blotting of single chains.

FACS analysis of integrin and antigen expression

Levels of CD11b, CD16b and CD177 antigens as well as expression of $\alpha 5\beta 1$ and $\alpha v\beta 3$ integrins were determined by fluorescence-activated cell sorting (BD FACSAria II) [89]. Briefly, neutrophil-like cells ($5-10 \times 10^5$) were harvested and incubated with mouse monoclonal antibody anti-human CD11b conjugated with R-phycoerythrin (clone 2LPM19c, Dako), anti-human CD16b conjugated with APC (clone REA589, MiltenyiBiotec) or anti-human CD177 conjugated with FITC (clone REA258, MiltenyiBiotec) following manufacturers' instructions for 1 h at 4°C in the dark. Then, cells were washed with PBS and analyzed by flow cytometry. Three independent experiments were performed for each antibody. Similarly, K562 and K562 $\alpha v\beta 3$ cells (5×10^5) were incubated with 1

mg/ml mouse monoclonal antibodies HA5 and LM609 (Chemicon) recognizing $\alpha 5\beta 1$ and $\alpha v\beta 3$ integrins, respectively, for 1 h at 4°C in the dark. After washing with PBS, cells were incubated with FITC-conjugated anti-mouse IgG (Sigma-Aldrich), diluted 1:40, for 30 min at 4° C in the dark and then subjected to FACS using BD FACSDiva 8.0 software. Simultaneous representation of different histograms from the same cell line was obtained by Kaluza Flow Citometry analysis V1.2 (Beckman Coulter). Two independent experiments were performed for each cell line and antibody.

Western blot analysis of integrin expression

Whole cell lysates were obtained using standard protocol. Briefly, cells were washed in PBS and then lysed on ice in 100 μ l of RIPA lysis buffer (Tris-HCl pH 7.6, 150mM NaCl, 1% NP-40, 1% sodium deoxycholate, 0.1% SDS) with proteases and phosphatases inhibitors (Sigma-Aldrich). The suspension was then homogenized by passages through a 26-gauge needle and centrifuged at 15700xg for 30 min at 4°C. Western blot analysis of proteins from whole cell lysates was carried out using a standard procedure. Briefly, protein samples (40 μ g) were subjected to SDS-PAGE and then transferred to PVDF membranes. After blocking with 5% non-fat dry milk, membranes were probed by rabbit polyclonal antibodies (1:500) recognizing $\alpha 5$ (Chemicon), α I**I**b (Santa Cruz), $\beta 1$ (Chemicon), $\beta 3$ (Santa Cruz) and $\beta 5$ (Santa Cruz) chains whereas mouse monoclonal antibodies were used to probe αv chain (clone P2W7, 1:500, Santa Cruz) and actin (Sigma; 1 μ g/mL). A commercially available ECL kit (GE Healthcare) was used to reveal the reaction.

Qualitative and quantitative analysis of NETs

Fluorescence microscopy was used to evaluate NETs formation. Briefly, 5×10^5 neutrophil-like cells were seeded in 24-well tissue culture plates with glass coverslips in serum-free HBSS with calcium and magnesium chloride at 37°C with 5% CO₂ and allowed to attach. Then cells were treated with calcium ionophore and stained with Sytox Green cell-impermeable nucleic acid dye (5 μ M,

Invitrogen). After washing with PBS, each coverslip was mounted on glass slide and examined by fluorescence microscopy.

Quantitative analysis of NETs formation was performed with Sytox Green followed by plate reader assay. Briefly, 1×10^5 neutrophil-like cells were seeded in 96-well black plate in 100 μ l of serum-free HBSS with calcium and magnesium chloride and left for 1 h at 37°C, 5%CO₂. After treatment with 2.5 and 25 μ M A23187, Sytox Green was added at 5 μ M for 10 min in a humidified incubator. The fluorescence was then measured using a PerkinElmer Multimode Plate Reader with EnSpire Manager Software and the results were expressed as percentage of total DNA release considering fluorescence readout obtained from cells lysed with 2% (vol/vol) Triton X-100 as 100% DNA release. Three independent experiments in triplicates were performed.

Analysis of NETs protein components

Samples from conditioned media of A23187-treated neutrophil-like cells or cell-free isolated NETs were analyzed by western blotting or immunoprecipitation. Levels of citrullinated histone H3 (Cit H3) were assayed after DNase 1 treatment (40 UI/ml, Roche) for 15 min at room temperature followed by centrifugation at 400xg for 5 min at 4°C. Protein samples (50 μ g, if not differently indicated) were subjected to western blot analysis as described above. Primary antibodies were anti-citrullinated histone H3 (citrulline R2+R8+R17, Abcam), total anti-histone H3 (Abcam) and anti-MPO (clone 2C7, Abcam), anti-fibronectin (clone 10/fibronectin, BD Biosciences) and anti-vitronectin (clone VIT-2, Sigma) mouse monoclonal antibodies. Gels were stained with coomassie dye R-250 using ImperialTM protein stain (Thermo Fisher Scientific) to obtain SDS-PAGE patterns of protein content and ensure equal loading.

Proteins (1.5 mg) from conditioned media of unstimulated and A23187-stimulated neutrophil-like cells in RPMI 1640 with 10% FBS were incubated with 2.5 μ g/ml of anti-fibronectin mouse monoclonal antibody overnight at 4°C under gentle rotation. The immunoprecipitated proteins

recovered by EZview Red Protein A Affinity Gel (Sigma-Aldrich) beads were separated by SDS-PAGE and analyzed by immunoblotting using the indicated antibodies.

Co-immunolocalization studies by confocal microscopy

Co-immunolocalization studies were performed in the laboratory of Dr. Carriero at the National Cancer Institute of Naples using a 510 META LSM confocal microscopy (Carl Zeiss). Briefly, neutrophil-like cells (2×10^5) were seeded in serum-free HBSS and allowed to attach onto glass coverslip in 24-well flat-bottom plates for 1 h at 37°C. Then cells were treated with calcium ionophore A23187 (25 μ M) to induce NETs release. Cells were fixed in formalin (2.5%) for 10 min at 4°C and incubated with rabbit polyclonal anti-citrullinated histone H3 (10 μ g/ml) (Abcam) and mouse monoclonal anti-fibronectin (2.5 μ g/ml) (clone 10/fibronectin, BD Biosciences) antibodies alone or in combination for 1 h at room temperature in the dark. Parallel experiments were performed by incubating permeabilized cells (0.1% Triton X-100) with mouse monoclonal antibody recognizing myeloperoxidase (MPO) (10 μ g/ml, clone 2C7, Abcam). In an additional set of experiments glass coverslips were incubated overnight at 4°C with 5 μ g of cell-free isolated NETs and then subjected to co-immunolocalization study using anti-Cit H3, anti-MPO and anti-fibronectin antibodies as described. After washing with PBS containing 1% BSA, 1:700 goat Alexa Fluor 594 anti-rabbit IgG and 1:500 rabbit Alexa Fluor 488 anti-mouse IgG (Molecular Probes) were added for 45 min at room temperature in the dark. Then glass coverslips were washed twice with PBS, mounted with ProLong Gold Antifade Reagent (Invitrogen) and examined by confocal microscopy.

Cell adhesion assays to NETs

A panel of human cancer cell lines differentially expressing $\alpha 5\beta 1$, $\alpha v\beta 3$, $\alpha IIb\beta 3$ and $\alpha v\beta 5$ integrins, that is fibrosarcoma (HT-1080), glioblastoma (U-87 MG), non-small cell lung cancer (H1975),

prostate cancer (DU 145 and PC-3) and epidermoid carcinoma (A-431), was subjected to adhesion assays using NETs as adhesion substrate. Briefly, 24-well flat-bottom plates were incubated overnight at 4°C with 5 µg of NETs stock in 200 µl of PBS and with diluent or conditioned medium from unstimulated neutrophil-like cells as negative controls. After gentle washing with PBS and incubation with serum-free culture medium with 1% BSA for 1 h at room temperature, cells (3×10^5 cells/well) were added and allowed to adhere for 1h at 37°C. Nonadherent cells were then removed by washing each well with serum-free culture medium whereas adherent cells were trypsinized and counted. Data are expressed as percentage of adherent cells compared to the total number of added cells. As negative controls, cells were seeded onto NETs coated wells that had been pre-treated with DNase 1 (10000 UI/ml, Roche) for 15 min at room temperature. To test whether DNA digestion was optimal, samples of NETs suspension were incubated with DNase 1 (10000 UI/ml) for 15 min and 30 min at RT and then loaded on 1.5 % agarose gel (w/v) containing 1 µg/ml ethidium bromide. To evaluate the role of $\alpha 5\beta 1$ and $\alpha v\beta 3$ integrins in promoting cell adhesion to NETs, cells were pre-treated with 45 µg/ml for 1 h at 4 °C with anti- $\alpha 5\beta 1$ P1D6 (Abcam) or anti- $\alpha v\beta 3$ LM609 (Chemicon) mouse monoclonal blocking antibodies and then seeded onto NETs coated plates at the final antibody concentration of 15 µg/ml. In addition to screen the adhesion ability of different integrins to NETs, a panel of cells were pre-incubated with a cyclic RGD peptide (10 µM) for 1 h at 4°C and then added to NETs coated plates with a final peptide concentration of 3.3 µM. To test the adhesion properties of protein components of NETs, Proteinase K (1.8 mg/ml, Invitrogen) was added to pre-coated wells for 30 min at 37°C and then removed.

Each cell line was subjected to three independent adhesion assays, including all experimental conditions, using different NETs stocks. In K562 and K562 $\alpha v\beta 3$ cells, three additional adhesion assays were performed using NETs released from neutrophil-like cells stimulated in the absence of serum, i.e. in exogenous vitronectin and fibronectin-free conditions.

Statistical analysis

Statistical analysis was performed using the software MedCalc for Windows, version 10.3.2.0, (MedCalc Software, Mariakerke, Belgium). Data are expressed as mean \pm SD if not differently indicated. Unpaired Student's t test was used to compare means. A p value < 0.05 was considered statistically significant.

RESULTS

Characterization of neutrophil-like cells and NETs production

Human acute promyelocytic leukemia HL-60 cells were differentiated in neutrophil-like cells adding 1.3% DMSO to the culture medium for seven days. Morphological changes and neutrophil markers expression induced by differentiation were tested by May-Grunwald-Giemsa staining and by fluorescence activated cell sorting analysis using antibodies recognizing CD11b, CD16b and CD177 antigens. The mean percentages of neutrophil-like cells positively stained for CD11b, CD16b and CD177 were $60\% \pm 16\%$, $84\% \pm 19\%$ and $78\% \pm 16\%$, respectively.

Neutrophil-like cells were then treated with calcium ionophore A23187 to induce NETs release. The process of NETs formation was qualitatively and quantitatively evaluated by using Sytox Green nucleic acid dye. Figures 1 A and B show representative images of unstimulated and stimulated neutrophil-like cells obtained by fluorescence microscopy: positively stained web-like chromatin structures were found in the extracellular space of A23187-treated neutrophil-like cells (figure 1B) whereas they were absent in untreated cells (figure 1A). Furthermore, NETs and stimulated cells were positively stained for citrullinated histone H3 (Cit H3), a recognized marker of NETs structure (figure 1C).

Quantitative analysis of NETs formation was performed by Sytox green plate reader assay. Figure 1D shows a dose-dependent response of NETs formation induced by increasing concentration of

calcium ionophore. Considering fluorescence readout obtained from lysed cells as 100%, the percentage of extracellular DNA released by untreated cells was $29\% \pm 11\%$ whereas treatment of neutrophil-like cells with $2.5 \mu\text{M}$ and $25 \mu\text{M}$ of calcium ionophore caused $58\% \pm 14\%$ and $100\% \pm 1\%$ DNA release, respectively. These experiments showed that neutrophil-like cells treated with $25\mu\text{M}$ of A23187 are able to release the maximal amount of NETs.

Expression and co-immunolocalization of NETs markers

To confirm that released NETs contained Cit H3, western blot analysis was performed on samples of conditioned media from neutrophil-like cells treated or not with increasing concentrations of calcium ionophore A23187 and on samples from NETs stock. Figure 2A shows undetectable levels of Cit H3 in the conditioned medium of untreated cells whereas a dose-dependent increase of this marker was observed in response to A23187. As expected, even higher levels of Cit H3 were found in samples of cell-free isolated NETs obtained by centrifugation of conditioned media from stimulated cells whereas the protein was faintly detected in the corresponding samples from unstimulated cells (figure 2B). Similarly, high levels of myeloperoxidase (MPO) were found in the same samples (figure 2A) and to confirm co-immunolocalization of the two markers, simultaneous staining of Cit H3 (red) and MPO (green) was performed and analyzed by confocal microscopy both in the presence of neutrophil-like cells (figure 3, upper panels) and in cell-free suspension of NETs (figure 3, lower panels). Fusion images (yellow, upper and lower panels) showed that Cit H3 and MPO co-localize within NETs structure.

Adhesion of $\alpha 5\beta 1$ and $\alpha v\beta 3$ -expressing cells to NETs

To test whether expression of integrins $\alpha 5\beta 1$ and $\alpha v\beta 3$ may modulate cell adhesion to NETs, K562 and K562 $\alpha v\beta 3$ cells differentially expressing the two integrins were selected for cell adhesion assays to NETs. We preliminarily tested the expression of the two integrins in each cell line by

western blot analysis. Figure 4 shows that $\alpha 5$ and $\beta 1$ chains are equally expressed in both cell lines whereas αv and $\beta 3$ chains were expressed at high level only in K562 $\alpha v\beta 3$ cells stably cotransfected with cDNA of both chains. Levels of whole integrins were also tested by flow cytometry and the results are shown in figure 5. As expected, K562 cells endogenously expressed $\alpha 5\beta 1$ integrin whereas levels of $\alpha v\beta 3$ were undetectable in this cell line showing a fluorescence intensity similar to that of negative control (figure 5A). Conversely, K562 $\alpha v\beta 3$ cells expressed higher levels of $\alpha v\beta 3$ integrin as compared to $\alpha 5\beta 1$ antigen (figure 5B). Although the single chains $\alpha 5$ and $\beta 1$ were equally expressed in K562 and K562 $\alpha v\beta 3$ cells, the whole $\alpha 5\beta 1$ integrin was detected in $75\% \pm 19\%$ of K562 cells and in $10\% \pm 10\%$ of K562 $\alpha v\beta 3$ cells by FACS analysis using an antibody recognizing the whole integrin. This apparent discrepancy may be explained by the impaired assembly of $\alpha 5\beta 1$ integrin on the plasma membrane of K562 $\alpha v\beta 3$ due to the predominant expression of αv and $\beta 3$ chains in this cell line. The whole $\alpha v\beta 3$ integrin was indeed expressed in $94\% \pm 1\%$ of K562 $\alpha v\beta 3$. Cell adhesion assays on NETs coated plates were then performed in the presence or absence of DNase 1, blocking antibodies against $\alpha 5\beta 1$ or $\alpha v\beta 3$, alone or in combination with DNase 1, and Proteinase K. The optimal degradation of double-stranded DNA in samples of NETs exposed to DNase 1 treatment was confirmed by agarose gel electrophoresis (figure 6). DNA fragments of approximately 50-100 base pairs were found in DNase 1 treated samples whereas double-stranded DNA remained indigested at the loading site in untreated samples. Furthermore, quantitative analysis of the agarose gel by ImageJ software (NIH, Bethesda, MD, USA) showed that the percentage of sample degradation at 15 min and 30 min was 95% and 93%, respectively, as compared to the untreated sample.

Figure 7A shows that when K562 cells were added to NETs coated plates, the mean percentage of adherent cells (expressed as percentage of adherent cells over the total number of seeded cells) was $59\% \pm 8\%$. A statistically significant decrease of the percentage of adherent cells was observed after the addition of DNase 1 ($28\% \pm 1\%$, $p < 0.0001$) or anti- $\alpha 5\beta 1$ antibody ($24\% \pm 3\%$, $p < 0.001$) indicating that both nucleic acid and an integrin substrate were critical for cell adhesion to NETs.

Interestingly the combination of DNase 1 and anti- $\alpha 5\beta 1$ antibody almost completely blocked cell adhesion showing a mean percentage of adherent cells of $13\% \pm 1\%$ ($p=0.0001$). This value was significantly lower than that obtained with each agent alone (vs DNase, $p<0.0001$; vs anti- $\alpha 5\beta 1$, $p=0.0045$). Negative controls performed with PBS or conditioned medium of unstimulated neutrophil-like cells showed a mean cell adhesion of $7\% \pm 3\%$ and $5\% \pm 1\%$, respectively. Similarly, cell adhesion assays of K562 $\alpha v\beta 3$ cells to NETs coated plates showed $80\% \pm 3\%$ of adherent cells that significantly decreased to $17\% \pm 3\%$ in the presence of DNase 1 ($p<0.0001$) and to $17\% \pm 4\%$ when anti- $\alpha v\beta 3$ blocking antibody was added ($p<0.0001$, figure 7B). The combination of DNase 1 and anti- $\alpha v\beta 3$ antibody resulted in $11\% \pm 4\%$ of adherent cells, a value lower than that observed with DNase 1 ($p<0.05$) and anti- $\alpha v\beta 3$ antibody ($p=0.1017$) alone. Negative controls performed with PBS and conditioned medium of unstimulated neutrophil-like cells showed a mean cell adhesion of $4\% \pm 2\%$ and $9\% \pm 1\%$, respectively. In both K562 and K562 $\alpha v\beta 3$ cells, the addition of Proteinase K caused inhibition of cell adhesion ($p<0.05$ for K562 and $p<0.001$ for K562 $\alpha v\beta 3$) confirming the crucial role of the protein content of NETs structure in cell adhesion (figure 7 A and B). Similar results were obtained using NETs released from neutrophil-like cells stimulated in serum-free conditions, i.e. in exogenous vitronectin and fibronectin-free conditions (Table 1). In particular, a significant reduction of cell adhesion was observed after treatment with DNase 1 or anti-integrin antibody in both K562 (DNase 1, $p<0.01$; anti- $\alpha 5\beta 1$, $p<0.01$) and K562 $\alpha v\beta 3$ (DNase 1, $p<0.0001$, anti- $\alpha v\beta 3$, $p<0.0001$) cell lines. These experiments showed that both $\alpha 5\beta 1$ and $\alpha v\beta 3$ integrins are able to modulate adhesion of cancer cells to NETs.

Fibronectin is a protein component of NETs

Since both $\alpha 5\beta 1$ and $\alpha v\beta 3$ integrins bind with high affinity to fibronectin and vitronectin containing the RGD aminoacid sequence, we tested whether cell-free isolated NETs and conditioned media of stimulated and unstimulated neutrophil-like cells contained these integrin substrates. Western blot

analysis in figure 8A shows a dose-dependent increase of fibronectin levels in the conditioned medium of stimulated neutrophil-like cells whereas a faint fibronectin signal was observed in samples of conditioned medium from unstimulated cells using both standard and serum free conditions (i.e. in exogenous vitronectin and fibronectin-free conditions) (figure 8A, left and right panels, respectively). High levels of fibronectin were also found in samples of cell-free isolated NETs obtained by stimulating neutrophil-like cells in both standard and serum-free conditions (figure 8B, left and right panels, respectively) whereas the protein was undetectable in the corresponding negative control. Vitronectin levels were undetectable in all samples (figure 9). Immunoprecipitation of proteins from conditioned media of unstimulated and stimulated neutrophil-like cells showed an undetectable, faint or strong signal for fibronectin in samples from untreated, 2.5 μ M and 25 μ M of A23187 treated cells, respectively (figure 10). Furthermore, a strong signal for histone H3 was found only in conditioned medium of highly stimulated neutrophil-like cells indicating that fibronectin directly or indirectly interacts with histone H3 (figure 10). To test whether fibronectin is localized within NETs, co-immunolocalization studies of fibronectin and Cit H3 were performed using confocal microscopy in stimulated neutrophil-like cells and in NETs stock (figure 11). Representative images of NETs in the extracellular space of stimulated neutrophil-like cells (figure 11, upper and middle panels) positively stained with anti-fibronectin antibody (green) and with anti-Cit H3 antibody (red) and merged images showed a clear co-localization of the two proteins in the structure of NETs. Similar results were obtained in cell-free isolated NETs (figure 11, lower panels). These findings taken together confirmed that fibronectin is localized within NETs and modulates cell adhesion to NETs through the engagement of α 5 β 1 and α v β 3 integrins, providing mechanistic clues on the in vivo interaction of NETs with different types of cells expressing these integrins including peripheral blood or activated endothelial cells as well as cancer cells.

Integrin-dependent adhesion to NETs of different cancer cell lines

To investigate the ability of different RGD-binding integrins to mediate adhesion to NETs, a panel of human cancer cell lines with a variable expression of $\alpha 5\beta 1$, $\alpha v\beta 3$, $\alpha I I b\beta 3$ and $\alpha v\beta 5$ integrins was subjected to adhesion assays to NETs in the presence and absence of an excess of cyclic RGD peptide and compared to DNase 1 treated samples. The expression of each integrin chain was tested by western blotting in whole lysates of HT-1080, U-87 MG, DU 145, PC-3, H1975 and A-431 cells. Figure 12 shows representative images of western blot analysis. Levels of $\alpha 5$ were undetectable in A-431 cells and faintly detected in PC-3 whereas all other cell lines expressed this integrin chain. High expression of αv was found in all cell lines except A-431 cells whereas levels of $\alpha I I b$ chain were higher in U-87 MG, HT-1080 and H1975 cells than in DU 145, PC-3 and A-431 cells. Among all β chains analyzed, A-431 cells lacked $\beta 1$ chain whereas PC-3 cells showed only a faint signal for the same protein. Finally, $\beta 5$ expression was undetectable in U-87 MG cells whereas $\beta 3$ was found in all cell lines.

Table 2 reports the results of adhesion assays on NETs of each cell line in the presence or absence of DNase 1 or excess of cyclic RGD peptide. The addition of cyclic RGD peptide reduced adhesion of HT-1080 and U-87 MG cells to values similar to those obtained with DNase 1 treatment and unstimulated CM as negative control (figure 13). In H1975 cells, competition with cyclic RGD peptide caused a partial reduction of adhesion to NETs lower than that obtained with DNase 1 treatment (figure 13). It is worthy to note that HT-1080, U-87 MG and H1975 have a similar pattern of $\alpha 5\beta 1$, $\alpha v\beta 3$ and $\alpha I I b\beta 3$ expression indicating that these three integrins may contribute to adhesion to NETs depending on their relative affinity for fibronectin. An equivalent statistically significant reduction of adhesion was obtained by both cyclic RGD peptide and DNase 1 treatment in DU 145 cells that, however, remained higher than negative controls (figure 13). Finally PC-3 and A-431 cells showed the lowest NETs-dependent and integrin-dependent adhesion with values similar to negative controls in all conditions (figure 13). These data along with the results obtained

in K562 and K562 α v β 3 cells, indicate that the integrins having a major role in the adhesion to NETs are α 5 β 1 and α v β 3 since the low expression of α 5 β 1 in PC-3 and A-431 prevents cell adhesion to NETs whereas high levels of α v β 3 enhance cell adhesion to NETs.

DISCUSSION

Our study in K562 and K562 α v β 3 cells showed that α 5 β 1 and α v β 3 integrins mediate cell adhesion to NETs by binding to their common substrate fibronectin, which was found to co-localize with Cit H3 inside the web-like structure of NETs and to interact directly or indirectly with histone H3. Treatment with DNase 1 and blocking antibodies against α 5 β 1 and α v β 3 integrins inhibited cell adhesion to NETs and when used in combination almost completely blocked cell adhesion indicating that both DNA and fibronectin were relevant in determining cell attachment to NETs. From quantitative data of cell adhesion, it is conceivable that treatment with DNase 1 alone would digest DNA, disrupt the web-like structure of NETs and prevent the interaction of DNA/histone complexes with fibronectin thus inhibiting cell adhesion not only to DNA but also to fibronectin. Since treatment with blocking anti-integrin antibodies resulted in a reduction of cell adhesion similar to that obtained with DNase 1, it is likely that cell adhesion to NETs may start with integrin-binding to fibronectin that would attract cells near to DNA/histone complexes allowing a stable cell interaction with DNA.

NETs incubated with plasma were reported to bind to several plasma proteins including fibronectin, von Willebrand factor and fibrinogen [40]. In our experiments, fibronectin was originated from neutrophil-like cells, since its levels were faintly detected in the conditioned medium of unstimulated neutrophil-like cells and increased in a dose-dependent manner in response to A23187. It is unclear whether fibronectin enter the structure of NETs during their formation or simply binds to NETs in the extracellular space. In this respect, fibronectin was reported to have a

moderately high affinity for eukaryote double-stranded DNA and a DNA-binding domain was described in human plasma fibronectin [90].

Two distinct pathways of NETs formation have been reported in human neutrophils: the PMA-induced NOX-dependent [14, 91] and the calcium ionophore-induced NOX-independent mechanisms [23]. The end point of both mechanisms is chromatin decondensation associated with histone citrullination followed by extrusion of nuclear DNA into the extracellular environment. The process is dependent on the generation of reactive oxygen species (ROS) and the migration of the protease neutrophil elastase (NE) and myeloperoxidase (MPO) from granules to the nucleus. The disruption of nuclear membrane that occurs during the process leads to the coalescence of nucleoplasm and cytoplasm so that cytoplasmic proteins including fibronectin can bind to DNA/histone complexes.

Cellular fibronectin is synthesized by many cell types, including fibroblasts and endothelial cells. It is an old notion that neutrophils, in addition to carry receptors for fibronectin on their plasma membrane, are also able to synthesize and secrete fibronectin [92, 93] especially at inflammatory and tissue injury sites. Similarly, HL-60 cells are reported to secrete fibronectin and to acquire receptors for fibronectin during their differentiation along the granulocytic pathway [94]. The main implication of the presence of fibronectin in the web-like structure of NETs is that it provides specific binding sites for several integrins expressed on the plasma membrane of neutrophils, platelets, endothelial and cancer cells.

When we screened a panel of cancer cell lines endogenously expressing a variety of integrins for their ability to bind to NETs, we found that the concomitant expression of $\alpha 5\beta 1$, $\alpha v\beta 3$ and $\alpha IIb\beta 3$ was associated to an enhanced adhesion to NETs and the addition of an excess of cyclic RGD peptide inhibited such adhesion although to a different extent in each cell line. The maximal reduction of integrin-dependent adhesion to NETs was similar to that obtained after DNase 1 treatment confirming that both DNA and fibronectin were relevant in determining cell attachment to NETs. The partial inhibition of adhesion by cyclic RGD peptide in certain cell lines may be due to

suboptimal competition for integrins with low affinity for fibronectin such as $\alpha v\beta 5$ [95] or to the expression of other integrins not analyzed in the panel. The observation that low or undetectable levels of $\alpha 5\beta 1$ integrin prevents cell adhesion to NETs suggests that this integrin is relevant to promote a stable cell interaction with DNA by binding to fibronectin. It is conceivable that $\alpha 5\beta 1$ integrin serves to anchor cells to the web-like structure allowing their close interaction with DNA/histone complexes. Similarly, $\alpha 5\beta 1$ may cooperate with $\alpha v\beta 3$ and other integrins favoring their binding to fibronectin. In agreement with our observations a recent study reported that silencing of $\beta 1$ -integrin with targeted siRNA in A549 lung cancer cells caused a decrease of cell adhesion to NETs in liver sinusoids as assessed by intravital microscopy in a mouse model of metastatic dissemination [62].

Our findings taken together indicate that, in addition to mechanical trapping and aspecific adsorption of different cell types driven by DNA/histone complexes, integrin-mediated cell adhesion to NETs should be taken into account as a mechanism promoting cell-cell interactions at the interface with NETs. By preventing fibronectin binding to integrins, specific inhibitors or antibodies may disrupt such cell-cell interactions and impair homing of circulating cancer cells to specific sites of NETs accumulation thus reducing NETs-dependent metastatic dissemination.

REFERENCES

1. Coffelt SB, Wellenstein MD, de Visser KE. Neutrophils in cancer: neutral no more. *Nat Rev Cancer* 2016;16: 431-46.
2. Furze RC, Rankin SM. Neutrophil mobilization and clearance in the bone marrow. *Immunology* 2008;125: 281-8.
3. Mayadas TN, Cullere X, Lowell CA. The multifaceted functions of neutrophils. *Annu Rev Pathol* 2014;9: 181-218.
4. Herter JM, Rossaint J, Block H, Welch H, Zarbock A. Integrin activation by P-Rex1 is required for selectin-mediated slow leukocyte rolling and intravascular crawling. *Blood* 2013;121: 2301-10.
5. Phillipson M, Heit B, Colarusso P, Liu L, Ballantyne CM, Kubes P. Intraluminal crawling of neutrophils to emigration sites: a molecularly distinct process from adhesion in the recruitment cascade. *J Exp Med* 2006;203: 2569-75.
6. Gambardella L, Vermeren S. Molecular players in neutrophil chemotaxis--focus on PI3K and small GTPases. *J Leukoc Biol* 2013;94: 603-12.
7. Phillipson M, Kubes P. The neutrophil in vascular inflammation. *Nat Med* 2011;17: 1381-90.
8. Heit B, Tavener S, Raharjo E, Kubes P. An intracellular signaling hierarchy determines direction of migration in opposing chemotactic gradients. *J Cell Biol* 2002;159: 91-102.
9. Kolaczkowska E, Kubes P. Neutrophil recruitment and function in health and inflammation. *Nat Rev Immunol* 2013;13: 159-75.
10. Brinkmann V, Reichard U, Goosmann C, Fauler B, Uhlemann Y, Weiss DS, et al. Neutrophil extracellular traps kill bacteria. *Science* 2004;303: 1532-5.
11. Erpenbeck L, Schon MP. Neutrophil extracellular traps: protagonists of cancer progression? *Oncogene* 2017;36: 2483-90.

12. Urban CF, Ermert D, Schmid M, Abu-Abed U, Goosmann C, Nacken W, et al. Neutrophil extracellular traps contain calprotectin, a cytosolic protein complex involved in host defense against *Candida albicans*. *PLoS Pathog* 2009;5: e1000639.
13. Barrientos L, Marin-Esteban V, de Chaisemartin L, Le-Moal VL, Sandre C, Bianchini E, et al. An improved strategy to recover large fragments of functional human neutrophil extracellular traps. *Front Immunol* 2013;4: 166.
14. Fuchs TA, Abed U, Goosmann C, Hurwitz R, Schulze I, Wahn V, et al. Novel cell death program leads to neutrophil extracellular traps. *J Cell Biol* 2007;176: 231-41.
15. Martinod K, Wagner DD. Thrombosis: tangled up in NETs. *Blood* 2014;123: 2768-76.
16. Schauer C, Janko C, Munoz LE, Zhao Y, Kienhofer D, Frey B, et al. Aggregated neutrophil extracellular traps limit inflammation by degrading cytokines and chemokines. *Nat Med* 2014;20: 511-7.
17. Neumann A, Vollger L, Berends ET, Molhoek EM, Stapels DA, Midon M, et al. Novel role of the antimicrobial peptide LL-37 in the protection of neutrophil extracellular traps against degradation by bacterial nucleases. *J Innate Immun* 2014;6: 860-8.
18. Aleyd E, van Hout MW, Ganzvles SH, Hoeben KA, Everts V, Bakema JE, et al. IgA enhances NETosis and release of neutrophil extracellular traps by polymorphonuclear cells via Fc α receptor I. *J Immunol* 2014;192: 2374-83.
19. Papayannopoulos V, Metzler KD, Hakkim A, Zychlinsky A. Neutrophil elastase and myeloperoxidase regulate the formation of neutrophil extracellular traps. *J Cell Biol* 2010;191: 677-91.
20. Li P, Li M, Lindberg MR, Kennett MJ, Xiong N, Wang Y. PAD4 is essential for antibacterial innate immunity mediated by neutrophil extracellular traps. *J Exp Med* 2010;207: 1853-62.
21. Wang Y, Li M, Stadler S, Correll S, Li P, Wang D, et al. Histone hypercitullination mediates chromatin decondensation and neutrophil extracellular trap formation. *J Cell Biol* 2009;184: 205-13.

22. Yipp BG, Kubes P. NETosis: how vital is it? *Blood* 2013;122: 2784-94.
23. Douda DN, Khan MA, Grasmann H, Palaniyar N. SK3 channel and mitochondrial ROS mediate NADPH oxidase-independent NETosis induced by calcium influx. *Proc Natl Acad Sci U S A* 2015;112: 2817-22.
24. Yang H, Biermann MH, Brauner JM, Liu Y, Zhao Y, Herrmann M. New Insights into Neutrophil Extracellular Traps: Mechanisms of Formation and Role in Inflammation. *Front Immunol* 2016;7: 302.
25. Halverson TW, Wilton M, Poon KK, Petri B, Lewenza S. DNA is an antimicrobial component of neutrophil extracellular traps. *PLoS Pathog* 2015;11: e1004593.
26. Cortjens B, van Woensel JB, Bem RA. Neutrophil Extracellular Traps in Respiratory Disease: guided anti-microbial traps or toxic webs? *Paediatr Respir Rev* 2017;21: 54-61.
27. Delgado-Rizo V, Martinez-Guzman MA, Iniguez-Gutierrez L, Garcia-Orozco A, Alvarado-Navarro A, Fafutis-Morris M. Neutrophil Extracellular Traps and Its Implications in Inflammation: An Overview. *Front Immunol* 2017;8: 81.
28. Saitoh T, Komano J, Saitoh Y, Misawa T, Takahama M, Kozaki T, et al. Neutrophil extracellular traps mediate a host defense response to human immunodeficiency virus-1. *Cell Host Microbe* 2012;12: 109-16.
29. Iba T, Hashiguchi N, Nagaoka I, Tabe Y, Murai M. Neutrophil cell death in response to infection and its relation to coagulation. *J Intensive Care* 2013;1: 13.
30. Malachowa N, Kobayashi SD, Quinn MT, DeLeo FR. NET Confusion. *Front Immunol* 2016;7: 259.
31. Bai Y, Tong Y, Liu Y, Hu H. Self-dsDNA in the pathogenesis of systemic lupus erythematosus. *Clin Exp Immunol* 2017;
32. Garcia-Romo GS, Caielli S, Vega B, Connolly J, Allantaz F, Xu Z, et al. Netting neutrophils are major inducers of type I IFN production in pediatric systemic lupus erythematosus. *Sci Transl Med* 2011;3: 73ra20.

33. Kessenbrock K, Krumbholz M, Schonermarck U, Back W, Gross WL, Werb Z, et al. Netting neutrophils in autoimmune small-vessel vasculitis. *Nat Med* 2009;15: 623-5.
34. Lande R, Ganguly D, Facchinetti V, Frasca L, Conrad C, Gregorio J, et al. Neutrophils activate plasmacytoid dendritic cells by releasing self-DNA-peptide complexes in systemic lupus erythematosus. *Sci Transl Med* 2011;3: 73ra19.
35. Khandpur R, Carmona-Rivera C, Vivekanandan-Giri A, Gizinski A, Yalavarthi S, Knight JS, et al. NETs are a source of citrullinated autoantigens and stimulate inflammatory responses in rheumatoid arthritis. *Sci Transl Med* 2013;5: 178ra40.
36. Hu SC, Yu HS, Yen FL, Lin CL, Chen GS, Lan CC. Neutrophil extracellular trap formation is increased in psoriasis and induces human beta-defensin-2 production in epidermal keratinocytes. *Sci Rep* 2016;6: 31119.
37. Knight JS, Carmona-Rivera C, Kaplan MJ. Proteins derived from neutrophil extracellular traps may serve as self-antigens and mediate organ damage in autoimmune diseases. *Front Immunol* 2012;3: 380.
38. Brill A, Fuchs TA, Savchenko AS, Thomas GM, Martinod K, De Meyer SF, et al. Neutrophil extracellular traps promote deep vein thrombosis in mice. *J Thromb Haemost* 2012;10: 136-44.
39. Brinkmann V, Zychlinsky A. Neutrophil extracellular traps: is immunity the second function of chromatin? *J Cell Biol* 2012;198: 773-83.
40. Fuchs TA, Brill A, Duerschmied D, Schatzberg D, Monestier M, Myers DD, Jr., et al. Extracellular DNA traps promote thrombosis. *Proc Natl Acad Sci U S A* 2010;107: 15880-5.
41. Nakazawa D, Tomaru U, Yamamoto C, Jodo S, Ishizu A. Abundant neutrophil extracellular traps in thrombus of patient with microscopic polyangiitis. *Front Immunol* 2012;3: 333.
42. Altincicek B, Stotzel S, Wygrecka M, Preissner KT, Vilcinskas A. Host-derived extracellular nucleic acids enhance innate immune responses, induce coagulation, and prolong survival upon infection in insects. *J Immunol* 2008;181: 2705-12.

43. Kannemeier C, Shibamiya A, Nakazawa F, Trusheim H, Ruppert C, Markart P, et al. Extracellular RNA constitutes a natural procoagulant cofactor in blood coagulation. *Proc Natl Acad Sci U S A* 2007;104: 6388-93.
44. Ammollo CT, Semeraro F, Xu J, Esmon NL, Esmon CT. Extracellular histones increase plasma thrombin generation by impairing thrombomodulin-dependent protein C activation. *J Thromb Haemost* 2011;9: 1795-803.
45. Semeraro F, Ammollo CT, Morrissey JH, Dale GL, Friese P, Esmon NL, et al. Extracellular histones promote thrombin generation through platelet-dependent mechanisms: involvement of platelet TLR2 and TLR4. *Blood* 2011;118: 1952-61.
46. Massberg S, Grahl L, von Bruehl ML, Manukyan D, Pfeiler S, Goosmann C, et al. Reciprocal coupling of coagulation and innate immunity via neutrophil serine proteases. *Nat Med* 2010;16: 887-96.
47. von Bruhl ML, Stark K, Steinhart A, Chandraratne S, Konrad I, Lorenz M, et al. Monocytes, neutrophils, and platelets cooperate to initiate and propagate venous thrombosis in mice in vivo. *J Exp Med* 2012;209: 819-35.
48. Martinod K, Demers M, Fuchs TA, Wong SL, Brill A, Gallant M, et al. Neutrophil histone modification by peptidylarginine deiminase 4 is critical for deep vein thrombosis in mice. *Proc Natl Acad Sci U S A* 2013;110: 8674-9.
49. Hisada Y, Geddings JE, Ay C, Mackman N. Venous thrombosis and cancer: from mouse models to clinical trials. *J Thromb Haemost* 2015;13: 1372-82.
50. Demers M, Krause DS, Schatzberg D, Martinod K, Voorhees JR, Fuchs TA, et al. Cancers predispose neutrophils to release extracellular DNA traps that contribute to cancer-associated thrombosis. *Proc Natl Acad Sci U S A* 2012;109: 13076-81.
51. Brandau S, Dumitru CA, Lang S. Protumor and antitumor functions of neutrophil granulocytes. *Semin Immunopathol* 2013;35: 163-76.

52. Demers M, Wagner DD. Neutrophil extracellular traps: A new link to cancer-associated thrombosis and potential implications for tumor progression. *Oncoimmunology* 2013;2: e22946.
53. Donskov F. Immunomonitoring and prognostic relevance of neutrophils in clinical trials. *Semin Cancer Biol* 2013;23: 200-7.
54. Powell DR, Huttenlocher A. Neutrophils in the Tumor Microenvironment. *Trends Immunol* 2016;37: 41-52.
55. Albanesi M, Mancardi DA, Jonsson F, Iannascoli B, Fiette L, Di Santo JP, et al. Neutrophils mediate antibody-induced antitumor effects in mice. *Blood* 2013;122: 3160-4.
56. Rohrbach AS, Slade DJ, Thompson PR, Mowen KA. Activation of PAD4 in NET formation. *Front Immunol* 2012;3: 360.
57. Sionov RV, Fridlender ZG, Granot Z. The Multifaceted Roles Neutrophils Play in the Tumor Microenvironment. *Cancer Microenviron* 2015;8: 125-58.
58. Ho-Tin-Noe B, Carbo C, Demers M, Cifuni SM, Goerge T, Wagner DD. Innate immune cells induce hemorrhage in tumors during thrombocytopenia. *Am J Pathol* 2009;175: 1699-708.
59. Berger-Achituv S, Brinkmann V, Abed UA, Kuhn LI, Ben-Ezra J, Elhasid R, et al. A proposed role for neutrophil extracellular traps in cancer immunoediting. *Front Immunol* 2013;4: 48.
60. Cools-Lartigue J, Spicer J, McDonald B, Gowing S, Chow S, Giannias B, et al. Neutrophil extracellular traps sequester circulating tumor cells and promote metastasis. *J Clin Invest* 2013;
61. Park J, Wysocki RW, Amoozgar Z, Maiorino L, Fein MR, Jorns J, et al. Cancer cells induce metastasis-supporting neutrophil extracellular DNA traps. *Sci Transl Med* 2016;8: 361ra138.
62. Najmeh S, Cools-Lartigue J, Rayes RF, Gowing S, Vourzoumis P, Bourdeau F, et al. Neutrophil extracellular traps sequester circulating tumor cells via beta1-integrin mediated interactions. *Int J Cancer* 2017;140: 2321-30.
63. Abram CL, Lowell CA. The ins and outs of leukocyte integrin signaling. *Annu Rev Immunol* 2009;27: 339-62.

64. Avraamides CJ, Garmy-Susini B, Varner JA. Integrins in angiogenesis and lymphangiogenesis. *Nat Rev Cancer* 2008;8: 604-17.
65. Plow EF, Haas TA, Zhang L, Loftus J, Smith JW. Ligand binding to integrins. *J Biol Chem* 2000;275: 21785-8.
66. Lee YC, Jin JK, Cheng CJ, Huang CF, Song JH, Huang M, et al. Targeting constitutively activated beta1 integrins inhibits prostate cancer metastasis. *Mol Cancer Res* 2013;11: 405-17.
67. Barthel SR, Hays DL, Yazawa EM, Opperman M, Walley KC, Nimrichter L, et al. Definition of molecular determinants of prostate cancer cell bone extravasation. *Cancer Res* 2013;73: 942-52.
68. Seguin L, Desgrosellier JS, Weis SM, Cheresh DA. Integrins and cancer: regulators of cancer stemness, metastasis, and drug resistance. *Trends Cell Biol* 2015;25: 234-40.
69. Rolli M, Fransvea E, Pilch J, Saven A, Felding-Habermann B. Activated integrin alphavbeta3 cooperates with metalloproteinase MMP-9 in regulating migration of metastatic breast cancer cells. *Proc Natl Acad Sci U S A* 2003;100: 9482-7.
70. Sloan EK, Pouliot N, Stanley KL, Chia J, Moseley JM, Hards DK, et al. Tumor-specific expression of alphavbeta3 integrin promotes spontaneous metastasis of breast cancer to bone. *Breast Cancer Res* 2006;8: R20.
71. Carriero MV, Del Vecchio S, Capozzoli M, Franco P, Fontana L, Zannetti A, et al. Urokinase receptor interacts with alpha(v)beta5 vitronectin receptor, promoting urokinase-dependent cell migration in breast cancer. *Cancer Res* 1999;59: 5307-14.
72. Nieberler M, Reuning U, Reichart F, Notni J, Wester HJ, Schwaiger M, et al. Exploring the Role of RGD-Recognizing Integrins in Cancer. *Cancers (Basel)* 2017;9:
73. Dong Y, Li A, Wang J, Weber JD, Michel LS. Synthetic lethality through combined Notch-epidermal growth factor receptor pathway inhibition in basal-like breast cancer. *Cancer Res* 2010;70: 5465-74.
74. Schaffner F, Ray AM, Dontenwill M. Integrin alpha5beta1, the Fibronectin Receptor, as a Pertinent Therapeutic Target in Solid Tumors. *Cancers (Basel)* 2013;5: 27-47.

75. Roman J, Ritzenthaler JD, Roser-Page S, Sun X, Han S. alpha5beta1-integrin expression is essential for tumor progression in experimental lung cancer. *Am J Respir Cell Mol Biol* 2010;43: 684-91.
76. Bennett JS. Structure and function of the platelet integrin alphaIIb beta3. *J Clin Invest* 2005;115: 3363-9.
77. Bledzka K, Smyth SS, Plow EF. Integrin alphaIIb beta3: from discovery to efficacious therapeutic target. *Circ Res* 2013;112: 1189-200.
78. Durrant TN, van den Bosch MT, Hers I. Integrin alphaIIb beta3 outside-in signaling. *Blood* 2017;
79. McCarty OJ, Zhao Y, Andrew N, Machesky LM, Staunton D, Frampton J, et al. Evaluation of the role of platelet integrins in fibronectin-dependent spreading and adhesion. *J Thromb Haemost* 2004;2: 1823-33.
80. Ruggeri ZM. Platelets in atherothrombosis. *Nat Med* 2002;8: 1227-34.
81. Erpenbeck L, Schon MP. Deadly allies: the fatal interplay between platelets and metastasizing cancer cells. *Blood* 2010;115: 3427-36.
82. Carrigan SO, Wepler AL, Issekutz AC, Stadnyk AW. Neutrophil differentiated HL-60 cells model Mac-1 (CD11b/CD18)-independent neutrophil transepithelial migration. *Immunology* 2005;115: 108-17.
83. Wang Y, Wysocka J, Sayegh J, Lee YH, Perlin JR, Leonelli L, et al. Human PAD4 regulates histone arginine methylation levels via demethylination. *Science* 2004;306: 279-83.
84. Millius A, Weiner OD. Chemotaxis in neutrophil-like HL-60 cells. *Methods Mol Biol* 2009;571: 167-77.
85. Nupponen I, Andersson S, Jarvenpaa AL, Kautiainen H, Repo H. Neutrophil CD11b expression and circulating interleukin-8 as diagnostic markers for early-onset neonatal sepsis. *Pediatrics* 2001;108: E12.

86. Di Fulvio M, Frondorf K, Henkels KM, Grunwald WC, Jr., Cool D, Gomez-Cambronero J. Phospholipase D2 (PLD2) shortens the time required for myeloid leukemic cell differentiation: mechanism of action. *J Biol Chem* 2012;287: 393-407.
87. Hickey MJ. Has Ly6G finally found a job? *Blood* 2012;120: 1352-3.
88. Butler B, Williams MP, Blystone SD. Ligand-dependent activation of integrin alpha v beta 3. *J Biol Chem* 2003;278: 5264-70.
89. Zannetti A, Del Vecchio S, Iommelli F, Del Gatto A, De Luca S, Zaccaro L, et al. Imaging of alpha(v)beta(3) expression by a bifunctional chimeric RGD peptide not cross-reacting with alpha(v)beta(5). *Clin Cancer Res* 2009;15: 5224-33.
90. Pande H, Calaycay J, Hawke D, Ben-Avram CM, Shively JE. Primary structure of a glycosylated DNA-binding domain in human plasma fibronectin. *J Biol Chem* 1985;260: 2301-6.
91. Remijsen Q, Vanden Berghe T, Wirawan E, Asselbergh B, Parthoens E, De Rycke R, et al. Neutrophil extracellular trap cell death requires both autophagy and superoxide generation. *Cell Res* 2011;21: 290-304.
92. La Fleur M, Beaulieu AD, Kreis C, Poubelle P. Fibronectin gene expression in polymorphonuclear leukocytes. Accumulation of mRNA in inflammatory cells. *J Biol Chem* 1987;262: 2111-5.
93. Hoffstein ST, Weissmann G, Pearlstein E. Fibonectin is a component of the surface coat of human neutrophils. *J Cell Sci* 1981;50: 315-27.
94. Pommier CG, O'Shea J, Chused T, Takahashi T, Ochoa M, Nutman TB, et al. Differentiation stimuli induce receptors for plasma fibronectin on the human myelomonocytic cell line HL-60. *Blood* 1984;64: 858-66.
95. Smith JW, Vestal DJ, Irwin SV, Burke TA, Cheresh DA. Purification and functional characterization of integrin alpha v beta 5. An adhesion receptor for vitronectin. *J Biol Chem* 1990;265: 11008-13.

TABLES

Table 1. Adhesion of K562 and K562 α v β 3 cells to NETs isolated in serum-free conditions

	K562 cells	K562αvβ3 cells
PBS	11% \pm 7%	6% \pm 1%
Unstimulated CM	7% \pm 4%	4% \pm 2%
NETs coated	62% \pm 14%	61% \pm 1%
+ DNase 1	10% \pm 7%	10% \pm 2%
+ anti-integrin blocking Ab	10% \pm 3%	8% \pm 3%
+ DNase 1 + anti-integrin blocking Ab	6% \pm 3%	5% \pm 2%
+ Proteinase K	21% \pm 4%	19% \pm 4%

Adhesion of K562 and K562 α v β 3 cells to NETs obtained from neutrophil-like cells stimulated with 25 μ M A23187 in serum free conditions, i.e. in exogenous vitronectin and fibronectin-free conditions. Data are expressed as percentage of adherent cells compared to the total number of added cells and the mean \pm SD of three independent experiments is reported for each condition.

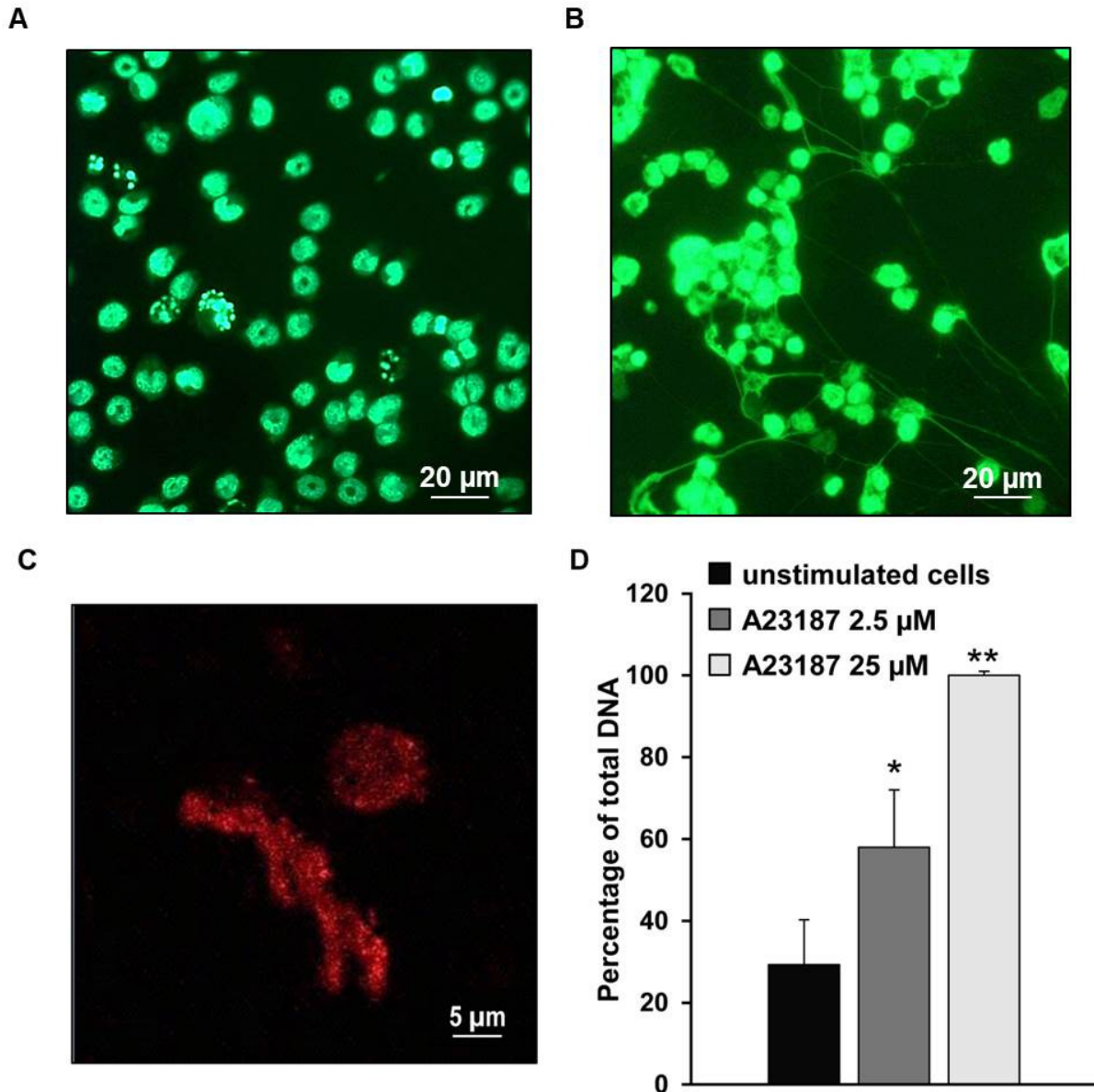
Table 2. Adhesion assay to NETs of HT-1080, U-87 MG, H1975, DU 145, PC-3 and A-431 cells

	PBS	Unstimulated CM	NETs coated	NETs coated + DNase 1	NETs coated + cyclic RGD peptide
HT-1080	38% \pm 6%	47% \pm 6%	101% \pm 2%	49% \pm 1%	59% \pm 2%
U-87 MG	31% \pm 4%	42% \pm 3%	99% \pm 12%	64% \pm 10%	65% \pm 14%
H1975	15% \pm 8%	30% \pm 9%	66% \pm 8%	37% \pm 8%	57% \pm 8%
DU 145	2% \pm 1%	9% \pm 3%	50% \pm 4%	25% \pm 5%	33% \pm 3%
PC-3	21% \pm 3%	24% \pm 3%	39% \pm 8%	30% \pm 3%	28% \pm 2%
A-431	65% \pm 11%	61% \pm 11%	57% \pm 17%	56% \pm 9%	46% \pm 12%

Adhesion assay of integrins-expressing HT-1080, U-87 MG, H1975, DU 145, PC-3 and A-431 human cancer cell lines using cell-free isolated NETs as substrate. The results represent the mean \pm SE of three independent experiments and are expressed as percentage of adherent cells compared to the total number of plated cells.

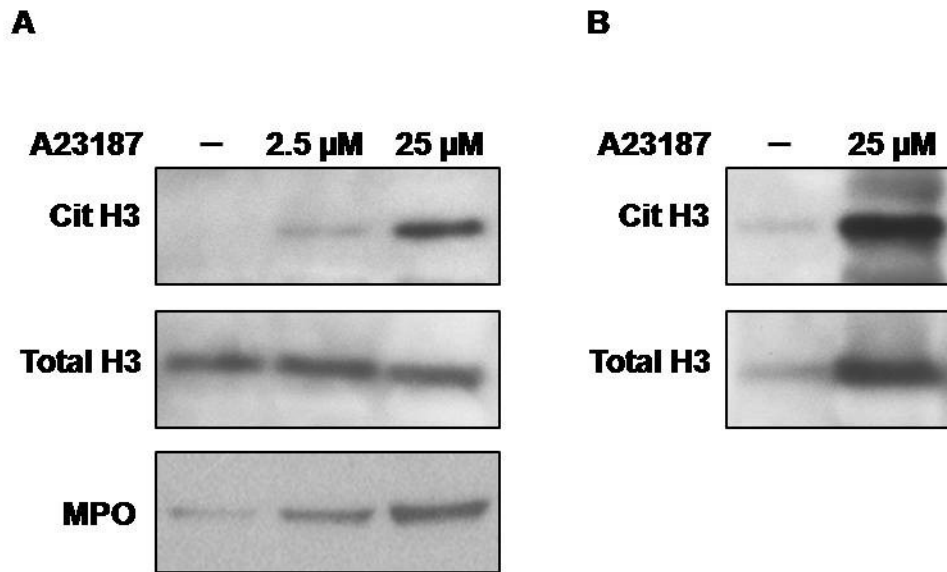
FIGURES

Figure 1. Qualitative and quantitative analysis of NETs formation induced by treatment of neutrophil-like cells with A23187



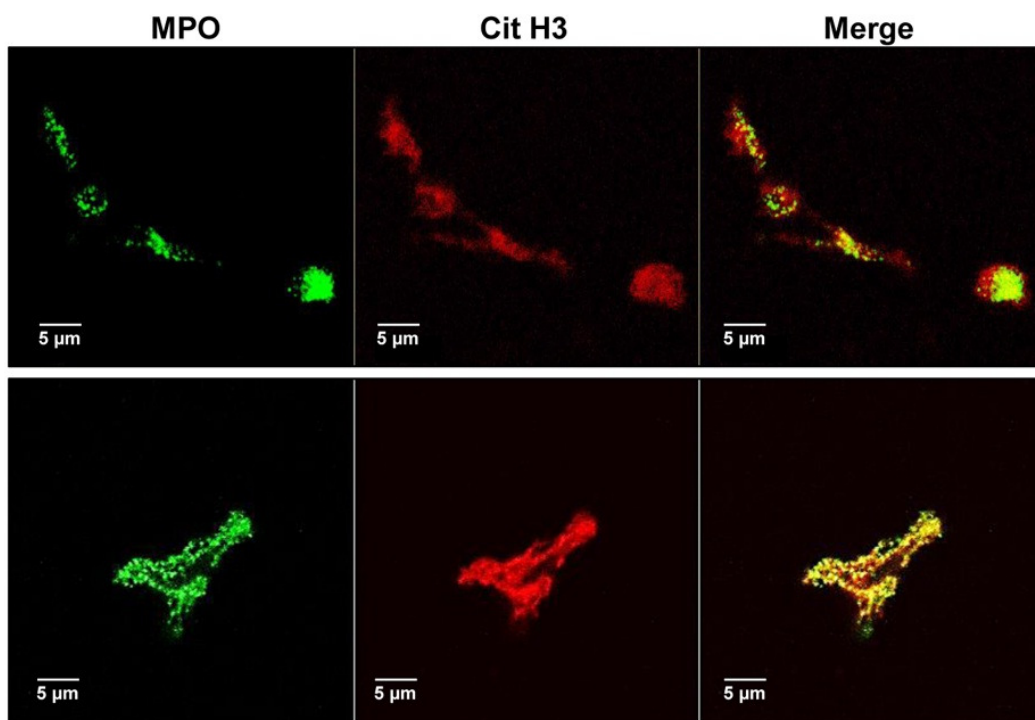
Representative images obtained by fluorescence microscopy of neutrophil-like cells stained with Sytox Green cell-impermeable nucleic acid dye in basal conditions (A) and after stimulation with 25 μM A23187 for 4 h. Scale bar, 20 μm (B). Representative image obtained by fluorescence microscopy at higher magnification showing morphological details of NETs stained with antibody recognizing Cit H3. Scale bar, 5 μm (C). Results of three independent fluorescence plate reader assays in unstimulated and stimulated neutrophil-like cells expressed as percentage of total DNA released from lysed cells (D).

Figure 2. Levels of citrullinated histone H3, total histone H3 and myeloperoxidase in NETs



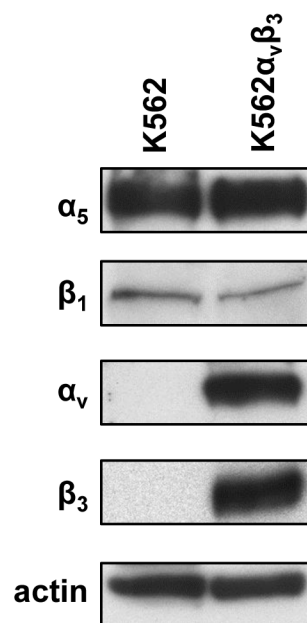
Western blot analysis of citrullinated histone H3 (Cit H3), total histone H3 (Total H3) and myeloperoxidase (MPO) in samples of NETs-enriched conditioned media (A) and cell-free isolated NETs (B) compared to the corresponding negative control.

Figure 3. Co-localization of citrullinated histone H3 and myeloperoxidase in NETs



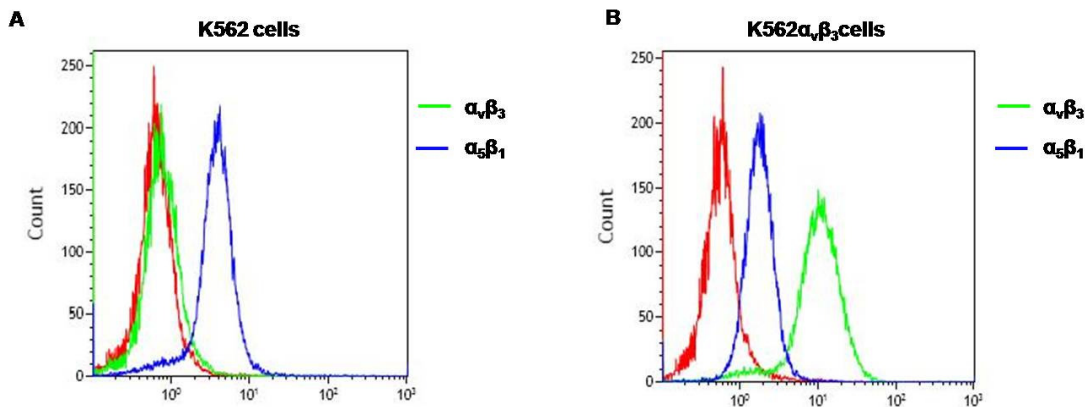
Representative images obtained with confocal microscopy showing co-localization of MPO (green) and Cit H3 (red) in neutrophil-like cells stimulated in serum-free conditions with 25 μ M A23187 for 4 h (upper panels) or in cell-free isolated NETs (lower panels). Merged images (yellow) showed the co-localization of MPO and Cit H3 confirming the typical features of NETs.

Figure 4. Levels of α_5 , β_1 , α_v and β_3 single chain expression in K562 and K562 $\alpha_v\beta_3$ cells by western blotting



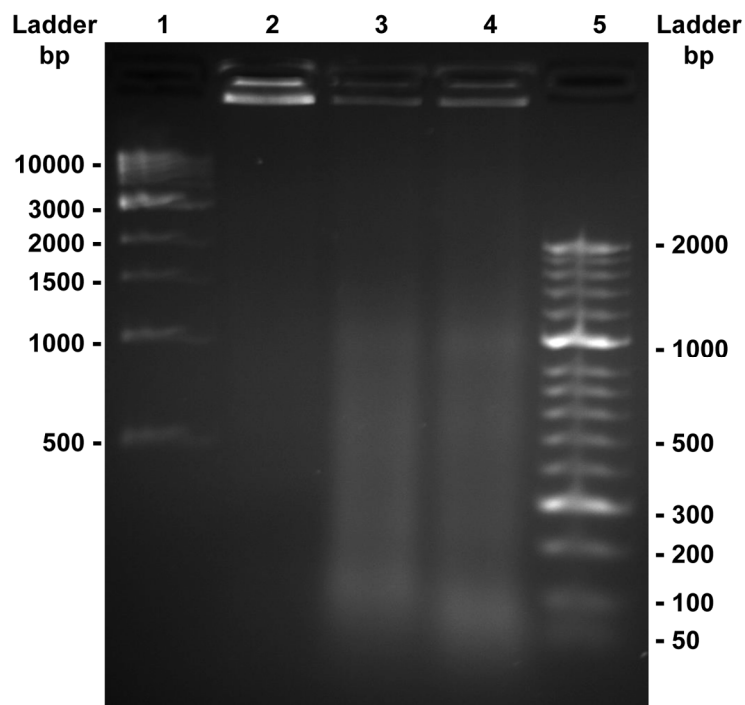
Samples of whole cell lysates (40 μ g of proteins) from K562 and K562 $\alpha_v\beta_3$ cells were subjected to western blot analysis using anti- α_5 (Chemicon), anti- β_1 (Chemicon), anti- β_3 (Santa Cruz) rabbit polyclonal antibodies and anti- α_v (clone P2W7, Santa Cruz) mouse monoclonal antibody. Actin ensured equal loading of samples.

Figure 5. Relative levels of $\alpha 5\beta 1$ and $\alpha v\beta 3$ integrins expression in K562 and K562 $\alpha v\beta 3$ cells by FACS



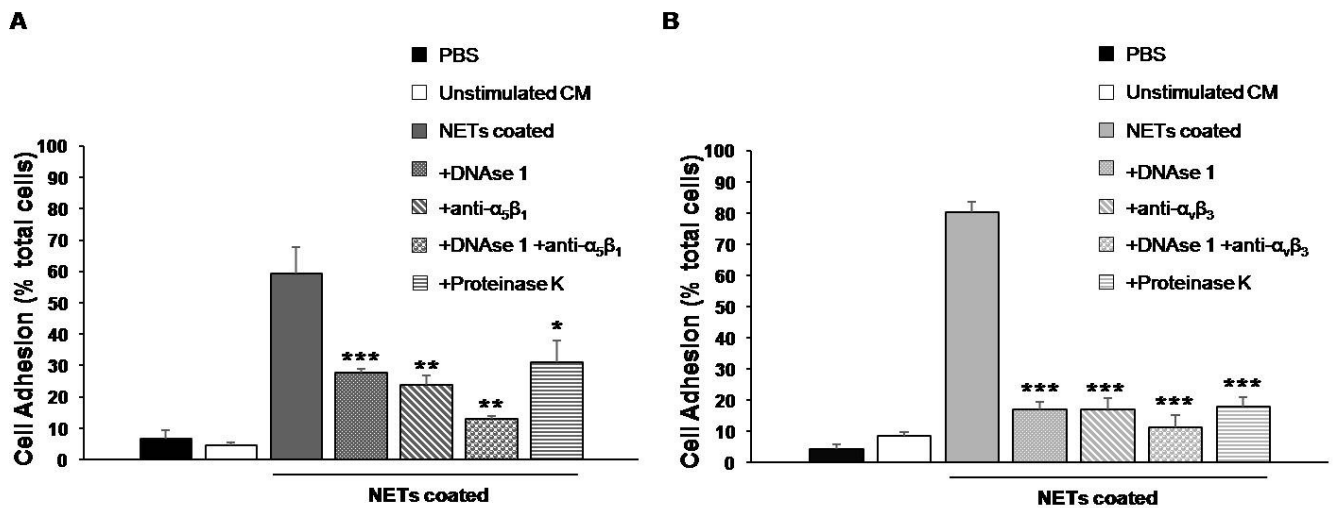
Simultaneous representation of different histograms from the same cell line obtained by Kaluza Flow Cytometry analysis V1.2 (Beckman Coulter). Expression of $\alpha 5\beta 1$ and $\alpha v\beta 3$ integrins in human K562 cells (A) and its derived clone K562 $\alpha v\beta 3$ (B) were determined by flow cytometry analysis using primary monoclonal antibodies HA5 (blue histograms) and LM609 (green histograms) recognizing $\alpha 5\beta 1$ and $\alpha v\beta 3$ integrins, respectively, and compared to the corresponding negative control (red histograms). Two independent experiments were performed for each cell line and antibody.

Figure 6. DNA degradation of NETs samples by DNase 1 treatment



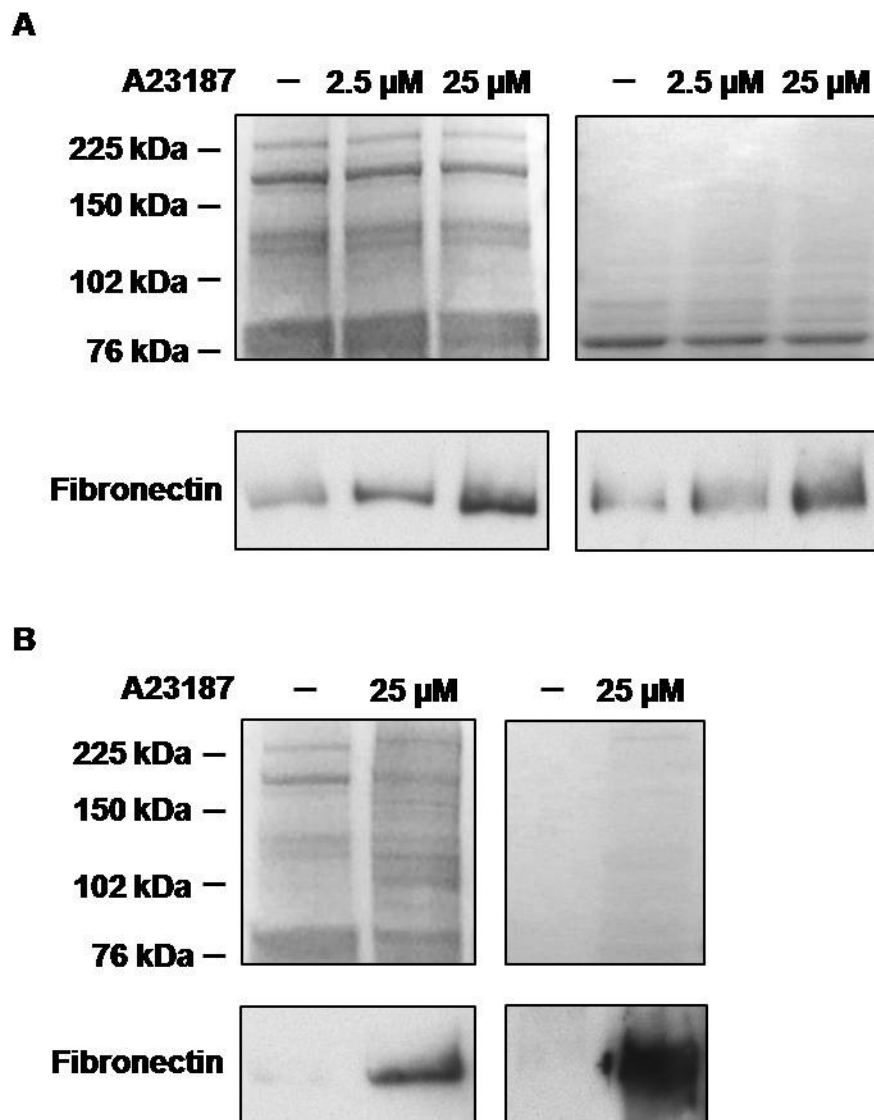
Samples of cell-free isolated NETs were incubated with DNase 1 (10000 UI/ml) for 15 min and 30 min at room temperature and then loaded on 1.5 % agarose gels (w/v) prepared in Tris-borate-EDTA buffer containing 1 µg/ml ethidium bromide. NETs DNA samples (8 µg) treated with DNase 1 for 15 min (lane 3) or 30 min (lane 4) showed the same smearing pattern along the gel whereas the untreated NETs sample (1 µg) did not show the presence of DNA fragments and remained undigested at the loading site (lane 2). Lane 1 and 5 show DNA molecular weight markers (ladder base pairs).

Figure 7. Adhesion of K562 and K562 α v β 3 cells to NETs



Results of adhesion assay of K562 and K562 α v β 3 are expressed as percentage of adherent cells compared to the total number of added cells and for each condition is reported the mean \pm SD of three independent experiments performed using different NETs stocks obtained from the stimulation of newly differentiated HL-60 cells in the presence of 10% FBS. Statistical significant differences between NETs coated and each experimental condition are indicated by symbols *, ** and ***, meaning $p < 0.05$, $p < 0.01$ and $p < 0.001$, respectively.

Figure 8. Protein levels of fibronectin in NETs



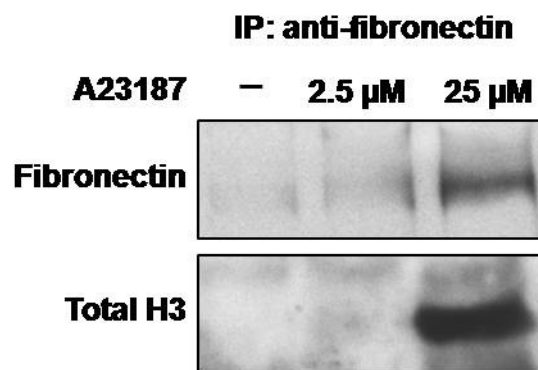
Levels of fibronectin were determined by Western blot analysis performed on samples of conditioned media of neutrophil-like cells stimulated or not with increasing concentration of A23187 in the presence (left panels, 50 μ g of protein per lane) or absence (right panels, 5 μ g of protein per lane) of serum (A). Results of western blotting on samples of NETs preparations obtained by stimulating neutrophil-like cells with 25 μ M A23187 for 4 h in the presence (left panels, 50 μ g of protein per lane) or absence (right panels, 5 μ g of protein per lane) of serum compared to the corresponding negative control from unstimulated cells (B). Gels were stained with Imperial protein stain to obtain SDS-PAGE patterns of protein content and ensure equal loading.

Figure 9. Western blot analysis of vitronectin expression in NETs



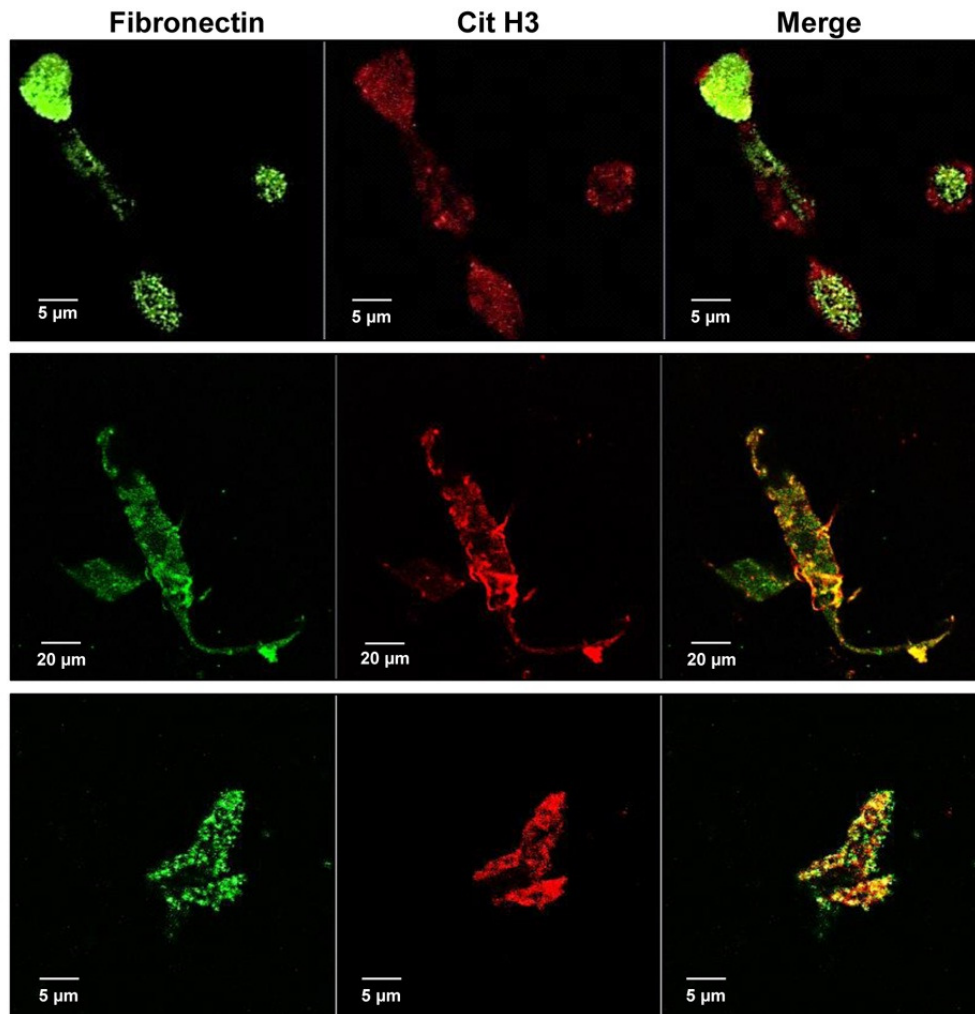
Samples of conditioned medium from unstimulated and stimulated neutrophil-like cells (A) or from cell-free isolated NETs (B) were subjected to western blot analysis (50 μ g of proteins) using an anti-vitronectin monoclonal antibody (clone VIT-2, Sigma) and purified vitronectin (Promega) as positive control. Vitronectin was undetectable in all samples except positive control.

Figure 10. Interaction between fibronectin and histone H3 in NETs



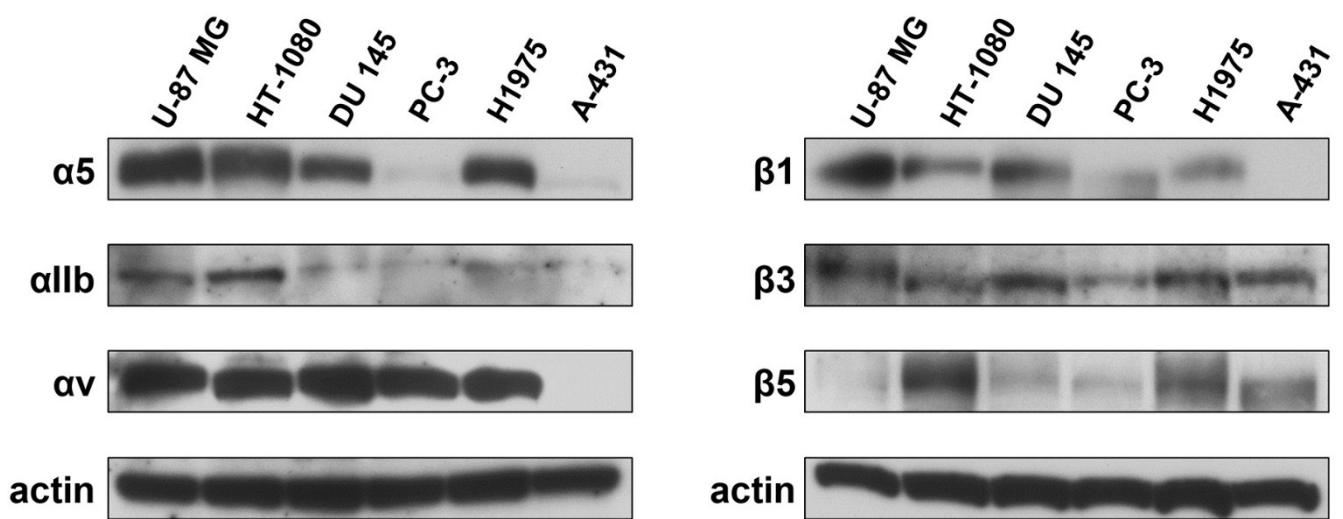
Immunoprecipitation of conditioned media from unstimulated and A23187-stimulated neutrophil-like cells was performed using anti-fibronectin antibody followed by SDS-PAGE of the immunoprecipitated proteins and immunoblotting with the indicated antibodies.

Figure 11. Co-localization of citrullinated histone H3 with fibronectin in NETs



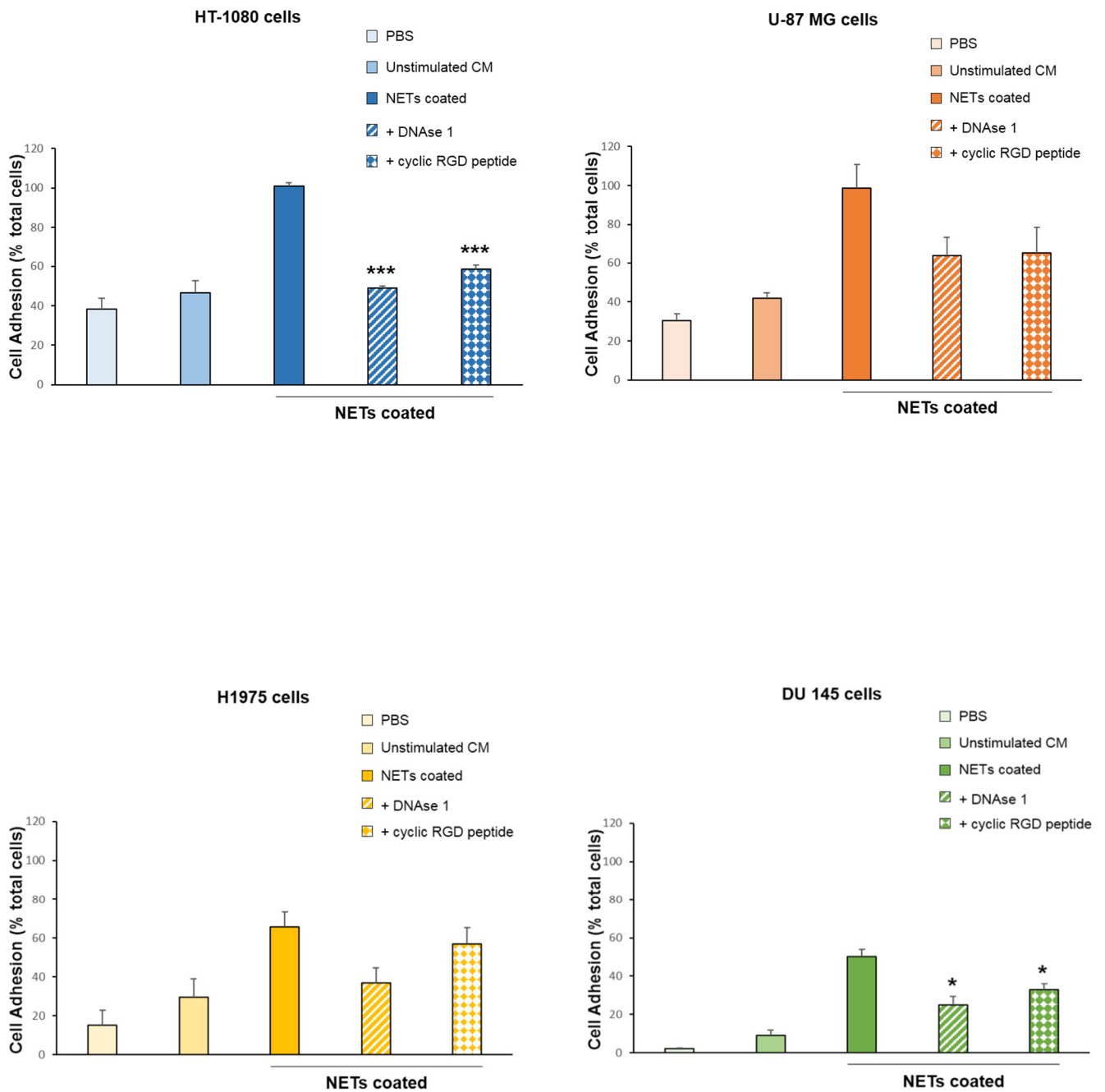
Representative images obtained with confocal microscopy showing co-localization of fibronectin (green) and Cit H3 (red) in neutrophil-like cells stimulated in serum-free conditions with 25 μ M of A23187 for 4 h (upper and middle panels) or in cell-free isolated NETs (lower panels). Merged images showed a clear co-localization of Cit H3 and fibronectin in the structure of NETs at early (upper panels) and late (middle panels) phases of the process coexisting in different fields as well as in NETs after their isolation procedures (lower panels).

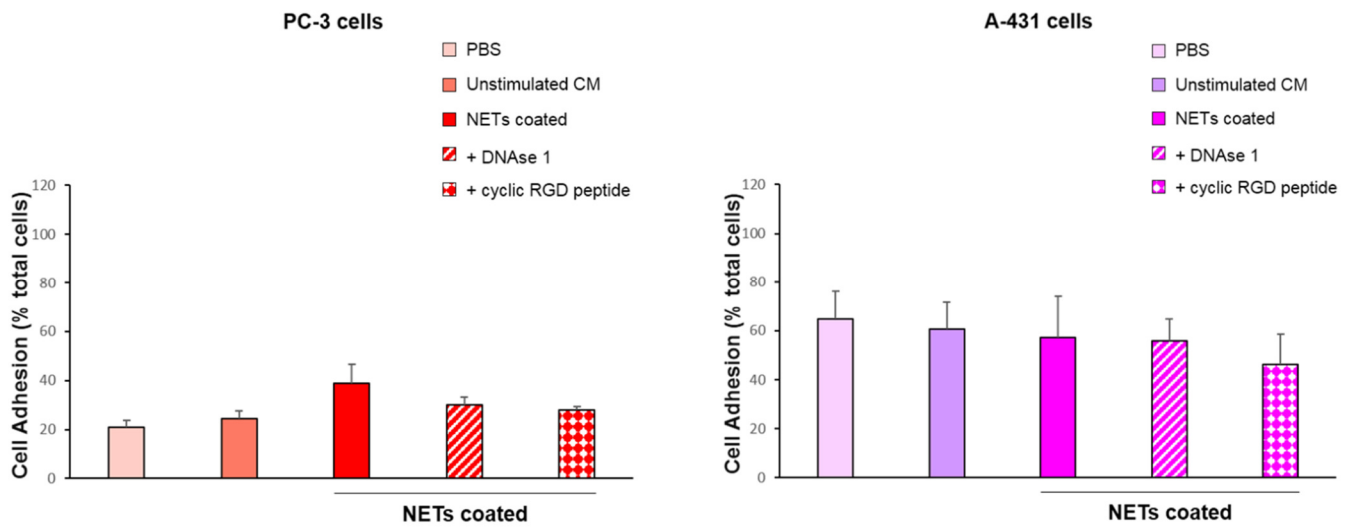
Figure 12. Protein expressions of $\alpha 5$, αIIb , αv , $\beta 1$, $\beta 3$ and $\beta 5$ chain integrin in U-87 MG, HT-1080, DU 145, PC-3, H1975 and A-431 cells



Western blotting of whole cell lysates from U-87 MG, HT-1080, DU 145, PC-3, H1975 and A-431 cells. Proteins (40 μ g) were separated by SDS-PAGE using 4-12% polyacrilamyide gels and PVDF membranes blotted with the indicated antibodies. Actin ensured equal loading.

Figure 13. Cell adhesion to NETs of integrins-expressing HT-1080, U-87 MG, H1975, DU 145, PC-3 and A-431 human cancer cell lines





Different cell-free isolated NETs were used to perform cell adhesion and obtain experimental replicates for each cell line tested. Results are expressed as percentage of adherent cells compared to the total number of added cells and the mean \pm SE of three independent experiments is reported for each condition. Statistical significant differences between NETs coated and each experimental condition are indicated by symbols *, ** and ***, meaning $p < 0.05$, $p < 0.01$ and $p < 0.001$, respectively.